Contrasting and conserved roles of NPR proteins in diverged land plant lineages

Hyung-Woo Jeon[1#], Hidekazu Iwakawa[1,6#], Satoshi Naramoto[2,7], Cornelia Herrfurth[3], Nora Gutsche[4], Titus Schlüter[1], Junko Kyozuka[2], Shingo Miyauchi[1], Ivo Feussner[3,5], Sabine Zachgo[4], Hirofumi Nakagami[1,8*]

[1]Max-Planck Institute for Plant Breeding Research, 50829 Cologne, Germany

[2]Graduate School of Life Sciences, Tohoku University, Sendai 980-8577, Japan

[3]Service Unit for Metabolomics and Lipidomics, Göttingen Center for Molecular Biosciences (GZMB), University of Göttingen, 37077 Göttingen, Germany

[4]Division of Botany, Osnabrück University, 49076 Osnabrück, Germany

[5]Department for Plant Biochemistry, Albrecht von Haller Institute for Plant Sciences and Göttingen Center for Molecular Biosciences (GZMB), University of Göttingen, 37077 Göttingen, Germany

[6]Present address: School of Biological Science and Technology, College of Science and Engineering, Kanazawa University, Kakuma-machi, Kanazawa 920-1192, Japan

[7]Present address: Department of Biological Sciences, Faculty of Science, Hokkaido University, Sapporo 060-0810, Japan

[8]Lead Contact

[#]equal contribution

[*]Correspondence: nakagami@mpipz.mpg.de

Telephone: +49-221-5062-224

Fax: +49-221-5062-353

ORCID

Hyung-Woo Jeon: 0000-0001-7587-6689

Hidekazu Iwakawa: 0000-0002-3362-9978

Satoshi Naramoto: 0000-0002-3373-6343

Cornelia Herrfurth: 0000-0001-8255-3255

Nora Gutsche: 0000-0002-8306-3087

Titus Schlüter: 0000-0001-8281-0565

Junko Kyozuka: 0000-0003-2242-7171

Shingo Miyauchi: 0000-0002-0620-5547

Ivo Feussner: 0000-0002-9888-7003

Sabine Zachgo: 0000-0002-6666-1499

Hirofumi Nakagami: 0000-0003-2569-7062

Summary

The NPR proteins AtNPR1 and AtNPR3/AtNPR4 function as salicylic acid (SA) receptors in the model eudicot *Arabidopsis thaliana*. AtNPR1 plays a central role in SA-induced transcriptional reprogramming and thus positively regulates disease resistance against a variety of pathogens. NPR homologs have been found in the genomes of nearly all land plant species sequenced to date, suggesting that the function of NPR in the SA-mediated response is conserved in land plants. However, we know relatively little about the molecular functions and physiological roles of NPR homologs in most plant species. Our phylogenetic analysis of 194 NPR proteins from 68 land plant species shows that NPR proteins can be classified into three significant clades: angiosperms NPR1/2, angiosperms NPR3/4, and non-seed plants NPR. Uniquely, in Brassicaceae species, NPR genes have been duplicated to form four Brassicaceae-specific subclades. Brassicaceae NPR1-like proteins have characteristically gained or lost functional amino acid residues or protein motifs identified in *A. thaliana* NPR proteins, pointing to the possibility of a unique evolutionary trajectory for the Brassicaceae NPR1-like proteins that has resulted in peculiar functions. We find that the only NPR in the model liverwort *Marchantia polymorpha*, MpNPR, is not the master regulator of SA-induced transcriptional reprogramming and rather negatively regulates resistance against bacterial pathogens in this species, although Mp*NPR* expression could complement the mutant phenotypes of At*npr1-1*. The transcriptome of Mp*npr* mutant plants suggested potential roles of MpNPR in heat and far-red (FR) light responses. Indeed, Mp*npr* mutants displayed enhanced thermomorphogenesis and reduced FR-induced shade avoidance. Furthermore, we identify enhanced thermomorphogenesis in At*npr1-1* seedlings, suggesting a conserved role of NPR in the heat response in land plants. Taken together, our results demonstrate that the SA-mediated disease resistance-related function of NPR is not evolutionarily well conserved among land plant lineages. We suggest that the common ancestor of land plants had acquired NPR to cope with highly fluctuating conditions, including temperature and light quality, in terrestrial environments.

Introduction

Land plants deal with various environmental fluctuations or stresses such as shadiness, heat, and drought. Likewise, land plants are constantly surrounded by various microbes and insects and have

64 developed sophisticated immune systems to fight off a wide range of pathogenic organisms. Plant
65 immune responses are controlled by diverse phytohormones such as salicylic acid (SA), jasmonic acid
66 (JA), and ethylene (ET), among which SA has indispensable roles in both local and systemic protection
67 against biotrophic and hemibiotrophic pathogens [1,2]. In *Arabidopsis thaliana*, NONEXPRESSOR OF
68 PATHOGENESIS-RELATED GENES1 (NPR1) is a central player in SA-mediated plant immunity.
69 AtNPR1 is responsible for the majority of SA- or benzothiadiazole S-methyl ester (BTH; a functional
70 analog of SA)-induced transcriptional reprogramming, positioning AtNPR1 as the master regulator of
71 the regulatory defense network induced by SA in *A. thaliana* [3,4]. Consistent with this, the controlled
72 expression of AtNPR1 in rice enhances resistance against bacterial and fungal pathogens without
73 compromising plant fitness [5], underlining the potential of NPR homologs as molecular targets or tools
74 for the engineering of disease-resistant plants.

75 AtNPR1 contains a Broad-complex, Tramtrack, and Bric-à-brac/poxvirus and zinc finger
76 (BTB/POZ) domain; Ankyrin repeats (ANKs); and a C-terminal NPR1-like-C domain [6–9]. The
77 genome of *A. thaliana* encodes four NPR proteins, AtNPR1, AtNPR2, AtNPR3, and AtNPR4. Besides,
78 *A. thaliana* has two BLADE-ON-PETIOLE (BOP) proteins, which are related to NPR proteins [10–12].
79 Although AtNPR2 is closely related to AtNPR1, the At*npr2* mutant behaves like a wild type in response
80 to SA, BTH, and bacterial pathogens [13]. However, expression of At*NPR2* can partially complement
81 the SA- and BTH-induced resistance phenotype of the At*npr1-1* mutant [13], suggesting functional
82 conservation between AtNPR1 and AtNPR2 as positive regulators of SA signaling. Meanwhile, the
83 At*npr3 npr4* double mutant displays enhanced resistance against bacterial and oomycete pathogens
84 associated with elevated basal pathogen-related (*PR*) gene expression, and AtNPR3 and AtNPR4 have
85 been shown to function as negative regulators of SA signaling [14,15].

86 AtNPR1, AtNPR3, and AtNPR4 have been demonstrated to function as SA receptors. The SA-
87 binding affinity of AtNPR proteins requires conserved arginine (Arg) residue in the C-terminal NPR1-
88 like-C domains [14,16,17]. An AtNPR1 mutant protein with the R432Q substitution failed to bind to
89 SA, and the At*npr1-1* mutant expressing this protein could not complement the SA-insensitivity
90 phenotype [14]. Similarly, *Brachypodium distachyon* NPR2, BdNPR2, was shown to possess SA
91 binding ability, which depends on the conserved Arg residue [18]. AtNPR3 and AtNPR4 can function

92 as transcriptional co-repressors, a function conferred by a repression motif, which is related to the
93 ethylene-responsive element binding factor (ERF)-associated amphiphilic repression (EAR) motif [19],
94 found at the C-terminal NPR1-like-C domains of AtNPR3 and AtNPR4 but not AtNPR1 [14]. Recent
95 structural analysis suggested that SA binding to AtNPR1 leads to formation of an "enhanceosome" [20].
96 The structural basis of how AtNPR3 and AtNPR4 function as transcriptional co-repressors remains to
97 be addressed.

98 AtNPR1 is a cysteine (Cys)-rich protein, and has been proposed to function as a redox sensor
99 [21]. In its inactive state, AtNPR1 forms oligomers through intermolecular disulfide bonds between Cys
100 residues that act to sequester the protein in the cytoplasm [22]. Importantly, Cys156 of AtNPR1 was
101 shown to be targeted by S-nitrosylation, which facilitates oligomerization [23]. Intriguingly, a recent
102 study indicated that the oligomerization of AtNPR1 reported to occur *in vitro* likely does not occur *in*
103 *vivo* [24]. Besides, AtNPR1, AtNPR3, and AtNPR4 were shown to regulate protein degradation by
104 recruiting the Cullin 3 E3 ubiquitin ligase, likely through their BTB/POZ domains [25].

105 The monophyletic bryophytes is a sister clade to tracheophytes [26–28]. The two plant lineages
106 diverged from the common ancestor of the land plants, which evolved from streptophyte algae about
107 500 million years ago [29,30]. Such taxonomic importance has placed bryophytes in a significant
108 position in the research of plant evolution and terrestrialization. Bryophytes consist of three divisions:
109 mosses, liverworts, and hornworts [31,32]. The genomes of model bryophytes, the moss *Physcomitrium*
110 *patens*, the liverwort *Marchantia polymorpha*, and the hornwort *Anthoceros agrestis*, encode two, one,
111 and no NPR homologs, respectively [27,33,34]. Notably, expression of *P. patens* Pp*NPR1*/Pp*3c21_7570*
112 can partially restore the *PR1* gene expression and disease resistance phenotypes of the At*npr1-1* mutant,
113 suggesting that the molecular properties of NPR proteins in bryophytes and angiosperms are
114 evolutionarily conserved at some level [35]. Accumulating evidence shows that ectopic expression of
115 At*NPR1* or NPR homologs in crops, including wheat, tomato, tobacco, and cotton, could alter disease
116 resistance, further supporting functional conservation of NPR proteins in many plant species [36–45].

117 Most genetic studies on *NPR* genes that have investigated their physiological roles in different
118 plant species have been carried out in *A. thaliana*. In one rare study in another plant species, in which
119 the authors employed RNAi-based Os*NPR1* knockdown lines in rice, it was reported that Os*NPR1* is

120 responsible for expression levels of 47% of BTH responsive genes [46]. However, it is not yet conclusive
121 whether OsNPR1 functions as the master regulator of SA signaling as in *A. thaliana*, because the study
122 was based on knockdown lines, and *O. sativa* has two other NPR proteins that may also contribute to
123 SA signaling [46]. Therefore, it is still possible that genes other than NPR factors play central roles in
124 SA signaling and that *NPR* genes primarily function in other pathways in plants. In this connection,
125 AtNPR1 was shown to positively regulate cold acclimation in SA- and TGA-independent manners [47].
126 Besides, AtNPR1 was described to suppress the unfolded protein response (UPR) independently from
127 SA by interacting with the UPR regulators bZIP28 and bZIP60 [48]. Here, we address the functional
128 conservation of NPR proteins in plants by utilizing the model liverwort *M. polymorpha* that possesses a
129 single NPR, MpNPR.
130
131 **Results**
132 *Brassicaceae NPR1-like proteins possess a peculiar set of functionally important amino acid residues*
133 Extensive studies of AtNPR proteins have identified protein motifs and amino acid residues
134 associated with the molecular mechanisms of how AtNPR proteins induce or repress the expression of
135 SA-responsive genes. To study functional conservation of NPR proteins across different plant species,
136 we performed comprehensive sequence analyses of NPR and BOP homologs. Amino acid sequences of
137 MpNPR (Mp1g02380) and AtBOP1 (At3g57130) were used for BLASTP search against 78 protein
138 databases covering algae, bryophytes, lycophytes, monilophytes, gymnosperms, and angiosperms
139 (Table S2). We identified 194 NPR and 123 BOP homologs in the genomes of 68 species covering the
140 significant lineages of land plants (Table S1). No NPR and BOP homologs were found in streptophyte
141 algae. We found that the exon-intron organization in the regions where the BTB/POZ domains are
142 encoded is highly conserved between NPR and BOP families (Figure S2). The phylogenetic tree shows
143 that NPR and BOP proteins from non-seed plants are closely related (Figure 1). This suggests that NPR
144 and BOP families diverged in the early stage of terrestrialization and may share a common ancestral
145 gene.
146 Phylogenetic analysis of 194 NPR proteins classified the NPR family into three significant
147 clades; Angiosperms NPR1/2, NPR3/4, and non-seed plants NPR (Figure 1A). The non-seed plants

148 clade consists entirely of NPR homologs from bryophytes and pteridophytes. NPR homologs from
149 angiosperms were clustered into the NPR1/2 and NPR3/4 clades, designated based on AtNPR1/AtNPR2
150 and AtNPR3/AtNPR4. The phylogenetic tree suggests that angiosperm NPR1/2 and NPR3/4 clades
151 diverged from the ancestral NPR by gene duplication (Figure 1A). Our comprehensive analysis,
152 including eight Brassicaceae species, revealed that *A. thaliana* gained a further four NPR proteins
153 through additional gene duplication that occurred after the divergence of the Brassicaceae family (Figure
154 1A). Consequently, NPR proteins from Brassicaceae species can be further classified into four
155 subclades: Brassicaceae NPR1-like to Brassicaceae NPR4-like (Figure 1A and S3B). Further expansions
156 of *NPR1-like* genes were observed in *Boechera stricta*, *Brassica rapa FPsc*, and *Eutrema salsugineum*,
157 while gene duplication of *NPR2-like*, *NPR3-like*, and *NPR4-like* was not observed except for *NPR3-like*
158 in *Brassica rapa FPsc* (Figure S3A). Intriguingly, one of the *Boechera stricta* NPR1-like proteins,
159 Bostr.29223s0069.1, was found to be integrated into the C-terminus of a Toll and IL-1 receptor (TIR)-
160 NLR (Figure S3C), which implies that Brassicaceae NPR1-like proteins are virulence targets of
161 pathogen effector molecules and, in turn, that, as supported by evidence from *A. thaliana*, Brassicaceae
162 NPR1-like proteins play crucial roles in plant immunity.

163 We then investigated the conservation of amino acids such as cysteine (Cys), serine (Ser), and
164 arginine (Arg) residues, which are associated with molecular functions of AtNPR1, together with
165 functional motifs including the EAR motif and SUMO-interaction motif (SIM) (Figure 1B to 1D and
166 S1). AtNPR1 forms an oligomer through intermolecular disulfide bonds in its inactive state to reside in
167 the cytoplasm, and several Cys residues were identified to be responsible for the oligomerization or
168 protein accumulation [22]. For instance, Cys156 is targeted by S-nitrosylation and is required for
169 AtNPR1 oligomerization [20,23]. Cys521 and Cys529 are critical for transition metal binding activity,
170 and oxidation is required for the SA-dependent co-activation activity of AtNPR1 [17,49]. We found that
171 Cys155 and Cys160, required for accumulation of AtNPR1 protein [22], were conserved in all 194 NPR
172 proteins (Figure 1B and S1). In contrast, Cys156 is conserved only in Brassicaceae NPR1-like and
173 NPR2-like subclades (Figure 1B and S1). Cys82 is involved in the oligomerization of AtNPR1 [20,22],
174 and we found that Cys82 is well conserved among NPR proteins in all clades and could be detected in
175 185 out of 194 NPR proteins (Figure S1). Cys521 and Cys529 are modestly conserved only in

176 Brassicaceae NPR1-like proteins (Figure S1). Arg432, required for SA binding in AtNPR1 [14], was
177 found to be well conserved among NPR proteins in all clades and was detected in 190 out of 194 NPR
178 proteins (Figure 1C and S1). The EAR motif (DLNxxP) of AtNPR3 and AtNPR4 was found to be
179 responsible for their transcriptional co-repressor activities [14]. Conversely, AtNPR1 was assumed to
180 function as a transcriptional co-activator due to the absence of this motif [50]. To our surprise, we found
181 that the EAR motif is conserved in most NPR proteins except for the Brassicaceae NPR1-like proteins
182 (Figure 1D and S1). Notably, the EAR motif is well conserved in Brassicaceae NPR2-like, NPR3-like,
183 and NPR4-like proteins (Figure S1). It is likely that Brassicaceae NPR1-like proteins have lost the EAR
184 motif during evolution. We observed occasional independent losses of the EAR motif in NPR proteins
185 from other plant species, including the single NPR in *M. polymorpha*, MpNPR (Figure 1D and Figure
186 S1). In short, Brassicaceae species have a unique set of NPR proteins, and Brassicaceae NPR1-like
187 proteins may have evolved unique molecular functions as positive regulators of SA-mediated immunity.
188

189 *NPR negatively regulates the SA response and resistance against bacterial pathogens in M.*
190 *polymorpha*

191 Based on the phylogenetic relationships of NPR proteins, functional characterization of NPR
192 proteins from bryophytes would be expected to shed light on the ancestral function of NPR and its
193 evolution. The acquisition of NPR has probably contributed to plant terrestrialization. However, the
194 absence of *NPR* genes in those hornworts for which genomes have been sequenced, namely, *Anthoceros*
195 *agrestis*, *Anthoceros punctatus*, and *Anthoceros angustus*, indicates that NPR is not indispensable for
196 the survival of plants in terrestrial environments. The model liverwort *M. polymorpha* has a single NPR,
197 which is an advantage for efforts aimed at addressing NPR functions. Since AtNPR1 plays a prominent
198 and vital role in SA responses in *A. thaliana*, a comparison of MpNPR and AtNPR1, both of which lack
199 the EAR motif, can contribute to understanding the conservation and diversification of NPR functions.
200 We thus generated CRISPR/Cas9-based NPR loss-of-function mutants in the *M. polymorpha* Tak-1
201 background. Two guide RNAs were used to target the first exon of Mp*NPR* near the region encoding
202 the BTB/POZ domain and resulted in 26-bp deletion (Mp*npr-1*^{ge}) and 1-bp insertion (Mp*npr-2*^{ge}),

203 respectively (Figure S4A). Both alleles resulted in a frameshift and early stop codons. We did not
204 observe obvious developmental defects of the Mp*npr* mutants under our growth conditions (Figure 2A).
205 SA was shown to inhibit the growth of *M. polymorpha*, and thus we first investigated SA
206 sensitivity of the Mp*npr* mutants [51]. Tak-1 plants showed no responses in their growth at
207 concentrations up to 0.5 mM SA, while both Mp*npr* mutants displayed growth inhibition only at 0.1
208 mM SA (Figure 2A and 2B). Complemented alleles expressing Mp*NPR* under its own promoter in
209 Mp*npr-1*^{ge} partially rescued the SA hypersensitivity phenotype (Figure 3A, 3B and S4B). Moreover,
210 Mp*NPR*-overexpressing plants, $_{pro}$Mp*EF1α::MpNPR-mCitrine/*Tak-1, displayed reduced sensitivity to
211 the SA treatment (Figure 3A and 3B). At*npr1* mutants are characterized by an SA-hypersensitive
212 phenotype due to hyperaccumulation of SA in these mutants [52]. Therefore, we next measured SA
213 levels in the Mp*npr* mutants to investigate whether the differential SA accumulation contributed to the
214 hypersensitive phenotype. Under our normal growth conditions, SA accumulated to the same levels in
215 the Tak1 and Mp*npr* mutants (Figure 2C). When plants were grown under SA-supplemented conditions,
216 we observed significantly lower and higher SA levels in Mp*npr-1*^{ge} and Mp*npr-2*^{ge} compared to Tak-1,
217 respectively. However, there was no correlation between the altered SA levels and the growth inhibition
218 phenotype (Figure 2A to 2C). In *M. polymorpha*, *dinor*-12-oxo-phytodienoic acid (dn-OPDA) functions
219 as bioactive jasmonate (JA), and antagonism between SA and dn-OPDA was reported [51,53,54].
220 Therefore, we also measured OPDA levels and found that these were not altered in the Mp*npr* mutants
221 (Figure 2D). Altogether, we concluded that MpNPR negatively regulates SA-dependent growth
222 inhibition.
223 AtNPR1 positively regulates SA-dependent defense gene expression, and thus At*npr1* mutants
224 display increased susceptibility to various bacterial pathogens [7,36,55]. Therefore, we investigated
225 whether and how MpNPR contributes to resistance against bacterial pathogens using recently
226 established pathosystems [56,57]. Two-week-old thalli of Tak-1 and Mp*npr* mutants were inoculated
227 with bioluminescent *Pseudomonas syringae* pv. *tomato* DC3000 (*Pto*-lux), and bacterial growth was
228 measured at 3 days post-inoculation (DPI). *Pto*-lux growth in the Mp*npr* mutants was significantly
229 reduced compared to the growth in Tak-1 both at basal and apical regions of thalli (Figure 2E).
230 Furthermore, the transient transformation of thalli with *Agrobacterium* carrying *intron-GUSPlus*

231 revealed that Mp*npr-1*^{ge} is more resistant to bacterial infection than Tak-1 (Figure 2F and 2G). These
232 results indicate that MpNPR negatively regulates bacterial resistance in *M. polymorpha*, which implies
233 that MpNPR and AtNPR1 play opposite roles in SA-mediated defense response.
234
235 *Molecular properties are conserved between MpNPR and AtNPR1*
236 Taking an inter-species complementation approach, we next determined whether the molecular
237 properties of NPR proteins from *M. polymorpha* and *A. thaliana* are conserved. Expression of At*NPR1-*
238 *mCitrine* under the Mp*EF1α* promoter in Mp*npr-1*^{ge} rescued the SA-hypersensitivity phenotype (Figure
239 3A and 3B). Moreover, $_{pro}$Mp*EF1α::*At*NPR1-mCitrine/*Mp*npr-1*^{ge} plants displayed reduced SA
240 sensitivity compared to Mp*NPR*-overexpressing plants, which is probably due to overaccumulation of
241 AtNPR1 (Figure 3A and 3B). Conversely, we expressed MpNPR under the cauliflower mosaic virus
242 (CaMV) 35S promoter in the At*npr1-1* mutant. Expression of Mp*NPR* and At*NPR1* rescued the SA
243 hypersensitive phenotype (Figure 3C). Line #4, which failed to express Mp*NPR*, was used as a control
244 (Figure 3C). The At*npr1-1* mutant possesses the GUS reporter, *BGL2::GUS*, that is responsive to SA
245 accumulation [58]. In plants treated with SA, GUS-staining was observed only in the complementation
246 lines (Figure 3D). Taken together, these results indicate that protein functions of MpNPR and AtNPR1
247 have been well conserved during evolution and that MpNPR can function as an SA receptor.
248
249 *MpNPR is not a master regulator of SA-induced transcriptional reprogramming in M. polymorpha*
250 In *A. thaliana*, the vast majority of SA-induced transcriptional reprogramming is governed by
251 AtNPR1, AtNPR3, and AtNPR4 [4]. Our results showing that in *M. polymorpha* there is potential only
252 a single SA receptor, MpNPR, would suggest that SA-induced transcriptional reprogramming will be
253 lost in the Mp*npr* mutants. To investigate the SA-induced transcriptional response in *M. polymorpha*
254 and the contributions of MpNPR to the response, 2-week-old Tak-1 and Mp*npr-1*^{ge} plants were treated
255 with 1 mM SA or Mock for 2, 6, and 12 hours and subjected to RNA-seq analysis (Figure S6A). The
256 number of differentially expressed genes (DEGs, Mock vs SA, $|\mathrm{Log_2FC}| \geq 1$, adjusted $p < 0.05$) in SA-
257 treated Tak-1 peaked at 6 hours post-incubation (hpi) (Figure 4B), and thus we selected a 6 hpi dataset
258 for further analyses. Strikingly, the overall transcriptional response pattern in Mp*npr-1*^{ge} was found to

259 be very similar to the pattern in Tak-1 (Figure 4A). Similar results were obtained when 7-day-old
260 gemmae, which were grown in a liquid medium, were treated with SA and BTH (Figure S7). This
261 indicates that the NPR protein is not a master regulator of SA-induced transcriptional reprogramming
262 in *M. polymorpha*. Since the transcriptional response was rather pronounced in Mp*npr-1*^{ge} compared to
263 Tak-1 (Figure 4B), MpNPR may rather function as a repressor of SA-inducible transcription factors,
264 which is in agreement with the SA hypersensitivity and the bacterial pathogen resistance phenotypes of
265 the Mp*npr* mutants (Figure 2). Moreover, this implies that other, as yet unknown, molecules likely
266 function as SA receptors in *M. polymorpha*.

267 In Tak-1, 479 genes were up-regulated and 97 genes were down-regulated upon SA treatment
268 (Figure 4B). Gene Ontology (GO) analysis showed significant enrichment of defense-related GO terms,
269 including '*response to wounding*' and '*response to other organism*', and also GO terms related to
270 responses to various stimuli in up- and down-regulated DEGs (Figure 4C). In Mp*npr-1*^{ge}, 837 genes
271 were up-regulated and 887 genes were down-regulated upon SA treatment (Figure 4B). Subsequent GO
272 analysis revealed that GO terms '*response to wounding*' is not enriched from the DEGs in Mp*npr-1*^{ge}
273 (Figure 4D). The expression of some Mp*PR* genes [59] was induced by SA treatment, and this up-
274 regulation was slightly enhanced in Mp*npr-1*^{ge} compared to Tak-1 (Figure S6C). These results imply
275 that SA is involved in the defense response and that MpNPR contributes to the SA-dependent wounding-
276 related response.

277

278 *MpNPR is involved in the heat and far-red light responses*

279 To explore the biological processes that are mediated by NPR but are independent of the SA
280 response in *M. polymorpha*, we compared the transcriptomes of Mp*npr-1*^{ge} and Tak-1 in response to
281 each treatment. Under Mock- and SA-treated conditions, 350 and 802 genes were identified as DEGs
282 (Mp*npr-1*^{ge} vs Tak-1, $|\mathrm{Log_2FC}| \geq 1$, adjusted $p < 0.05$), respectively (Figure 4E). Among the DEGs, 143
283 genes were shared in both Mock- and SA-treated conditions (Figure 4E and 4F). In this subset, 20 genes
284 showed significant changes in their expression patterns upon SA treatment (Figure 4F), and thus, we
285 defined 123 genes as MpNPR-dependent and SA-nonresponsive genes. Subsequent GO analysis

286 revealed that the biological processes '*response to heat*', '*response to temperature stimulus*', and
287 '*response to far red light*' are over-represented in these 123 genes (Figure 4G).

288 To examine whether MpNPR is involved in the response to heat, we grew plants at high ambient
289 temperatures, which was previously shown to induce folding and bending of *M. polymorpha* thalli as a
290 thermomorphogenic response [60]. As reported, enhanced three-dimensional (3D) growth of Tak-1
291 thalli was observed, resulting in reduced projected thallus area, when plants were grown at 30 °C (Figure
292 5A). The Mp*npr* mutants displayed enhanced folding and bending with smaller projected thallus area
293 compared to Tak-1 (Figure 5A), indicating that MpNPR negatively regulates thermomorphogenesis in
294 *M. polymorpha*. Then, we asked whether AtNPR1 also plays a role in thermomorphogenesis in *A.*
295 *thaliana*. Strikingly, we found that the At*npr1-1* mutant and the At*npr1-1 npr3-2 npr4-2* triple mutant
296 display enhanced hypocotyl elongation compared to a wild type Col-0 and the At*npr3-2 npr4-2* double
297 mutant at 28 °C but not at 22 °C (Figure 5B). The *pif4-101* mutant was used as a control (Figure 5B).
298 These results indicate that both MpNPR and AtNPR1 function as negative regulators of
299 thermomorphogenesis.

300 We further investigated the possible contribution of MpNPR to FR responses in *M. polymorpha*.
301 When plants were grown in a condition supplemented with FR light, enhanced upward growth of thalli
302 was observed, which is similar to shade avoidance responses in angiosperms (Figure 5C and 5D) [61–
303 63]. The Mp*PIF* knockout and overexpressing plants were used as controls (Figure 5C and 5D). We
304 found that Mp*npr* mutants display reduced upward growth compared to Tak-1 under the FR condition
305 (Figure 5C and 5D). The complemented allele displayed a trend toward rescuing the phenotype but was
306 not statistically significant (Figure 5C and 5D), which can be due to insufficient expression of MpNPR
307 in this plant compared to Tak-1 (Figure 3A and 5B). This observation supports the hypothesis that
308 MpNPR is involved in FR responses in *M. polymorpha*.

309

310 **Discussion**

311 Our phylogenetic analysis of 194 NPR proteins from 68 land plant species revealed that NPR
312 proteins from angiosperms can be classified into two paralogous clades, NPR1/2 and NPR3/4,
313 presumably diverged from an ancestral NPR (Figure 1). Two *NPR* genes were found in the genome of

314 *Amborella trichopoda*, the single extant species of the sister lineage to all other angiosperms, and these
315 genes, AmTr_v1.0_scaffold00036.47 and AmTr_v1.0_scaffold00032.72, were classified into the
316 NPR1/2 and NPR3/4 clades, respectively (Table S1). Meanwhile, NPR proteins from gymnosperms
317 formed a single cluster related to neither clade (Figure 1). This suggests that gene duplication of NPR
318 led to the emergence of the two paralogous clades, seemingly associated with the epsilon whole-genome
319 duplication (WGD) [64]. Interestingly, the analysis showed that the AtNPR1/AtNPR2 and
320 AtNPR3/AtNPR4 pairs most likely arose from a recent Brassicaceae-specific WGD event [65,66],
321 suggesting their functional redundancy in each clade. Indeed, AtNPR3 and AtNPR4 function
322 redundantly, and AtNPR2, but not AtNPR3 and AtNPR4, can complement At*npr1-1* mutant phenotypes
323 [13,15]. Moreover, rice OsNPR1/NH1 and cacao TcNPR1, which belong to the NPR1/2 clade, could
324 complement At*npr1* mutant phenotypes, and overexpression of OsNPR1/NH1 in rice resulted in
325 enhanced resistance against the bacterial pathogen *Xanthomonas oryzae* pv. *oryzae* [67]. This suggests
326 functional conservation among NPR proteins in the NPR1/2 clade. Similarly, cacao TcNPR3, which
327 belongs to the NPR3/4 clade, could complement At*npr3-3* mutant phenotypes, and CRISPR/Cas9-based
328 mutagenesis of *TcNPR3* in cacao resulted in enhanced resistance against the cacao pathogen
329 *Phytophthora tropicalis*, suggesting functionally conserved roles for NPR proteins in the NPR3/4 clade
330 as negative regulators of defense responses [68,69]. However, there is a contradictory report which
331 showed that overexpression of *Nicotiana glutinosa* NgNPR3, an AtNPR3 homolog, in *Nicotiana*
332 *tabacum* cv. Samsun enhanced resistance to *Alternaria alternata*, *Pseudomonas solanacearum*, and
333 potato virus Y [70]. Nevertheless, assuming that NPR proteins from the paralogous clades NPR1/2 and
334 NPR3/4 have acquired opposed or different functions, an obvious question arises of whether and how
335 NPR proteins in the non-seed plants clade, which can be remnants of NPR in the common ancestor of
336 land plants, play roles in SA signaling and defense responses. A single study reported that *P. patens*
337 PpNPR1 partially complements phenotypes of At*npr1-1* but not of At*npr3 npr4* [35]. Together with our
338 finding that AtNPR1 and MpNPR are interchangeable, it is likely that the molecular properties of non-
339 seed plant NPR proteins and NPR proteins in NPR1/2 clade are highly conserved during evolution. If
340 so, a remaining question is whether the molecular properties of NPR proteins in the NPR3/4 clade are
341 distinct from non-seed plant NPR proteins. Further genetic studies in many other plant species and inter-

342 species complementation assays will enhance our understanding of the functional conservation and
343 diversification of NPR proteins.

344 There is compelling evidence that AtNPR1 is the master regulator of SA- or BTH-induced
345 transcriptional reprogramming in *A. thaliana*. However, there is as yet no hint that other Brassicaceae
346 NPR1-like proteins or NPR proteins in the NPR1/2 clade also function as master regulators in their
347 respective species. In order to genetically engineer *NPR* genes to manipulate disease resistance, it is
348 crucial to understand the molecular functions of NPR proteins in other plant species. Further, it remains
349 unclear how AtNPR3 and AtNPR4 have evolved to become transcriptional co-repressors with opposite
350 roles to AtNPR1. One model that has been proposed is that the EAR motif located in the NPR1-like-C
351 domain of AtNPR3 and AtNPR4 differentiates them from AtNPR1, which lacks the EAR motif [14].
352 We found that the EAR motif found in AtNPR3 and AtNPR4 is perfectly conserved in all Brassicaceae
353 NPR2-like proteins, which suggests that Brassicaceae NPR2-like proteins can rather function as
354 transcriptional co-repressors instead of co-activators like AtNPR1. However, as mentioned above,
355 AtNPR2 was shown to complement At*npr1-1* mutant phenotypes. Conservation of the EAR motif in
356 Brassicaceae NPR2-like proteins suggested to us that AtNPR1 or Brassicaceae NPR1-like proteins have
357 presumably lost the EAR motif during evolution. To evaluate this hypothesis, we expanded our analysis
358 of functional protein sequences to all 194 NPR proteins. As expected, we found that the EAR motif is
359 widely conserved in NPR proteins from gymnosperms and all three major clades except for Brassicaceae
360 NPR1-like subclade (Figure S1). It is formally possible that other NPR proteins have acquired the EAR
361 motif independently during evolution, but we suggest that the more reasonable assumption is that
362 Brassicaceae NPR1-like proteins have lost the EAR motif after a Brassicaceae-specific WGD event. As
363 mentioned above, rice OsNPR1/NH1, cacao TcNPR1, and *P. patens* PpNPR1 could complement
364 phenotypes in At*npr1* mutants [35,67,71], and these three NPR proteins carry the EAR motif. These
365 observations indicate that the EAR motif is not by itself sufficient for the co-repressor or co-activator
366 function of NPR proteins. One plausible explanation could be that the EAR motif is controlled by
367 phosphorylation. We found that SP or TP sites in most NPR proteins of dicots in the NPR1/2 clade were
368 substituted with non-phosphorylable hydrophobic residues (A/V/L/I/M) (Figure S1). Although we have

369 no direct evidence that these sites are targeted by phosphorylation, these clade-specific mutations may
370 further explain how the EAR motif determines protein function.

371 The remarkable conservation of the Arg residue among NPR proteins, which is required for SA
372 binding in AtNPR1, AtNPR3, and AtNPR4 [14,16,17], seemingly suggests that NPR proteins generally
373 function as SA receptors in plants. However, unexpected conservation of the EAR motif made it difficult
374 for us to predict how NPR proteins coordinate the SA response in non- Brassicaceae plant species. Rice,
375 *O. sativa*, has three NPR proteins, OsNPR1/OsNH1, OsNPR2/OsNH2, and OsNPR3 [67], of which
376 OsNPR1/OsNH1 belongs to the NPR1/2 clade and OsNPR2/OsNH2 and OsNPR3 belong to the NPR3/4
377 clade (Figure S1). Overexpression of these three genes in rice suggested that only OsNPR1/OsNH1
378 functions as a positive regulator of defense responses [67], that is, OsNPR1/OsNH1 but not
379 OsNPR2/OsNH2 or OsNPR3, is a transcriptional co-activator of SA signaling. Accordingly, RNAi-
380 mediated knockdown of Os*NPR1* in rice resulted in impairment of BTH-induced transcriptional
381 reprogramming, but the observed impairment was not as striking as in At*npr1* mutants [46]. It is
382 important to generate and analyze Os*npr1* knockout plants, but there is a possibility that release of
383 transcriptional repression by OsNPR2/OsNH2 and OsNPR3 makes a large contribution to the SA
384 response. Analysis of a Os*npr1 npr2 npr3* triple mutant would clarify the contribution of NPR to SA
385 signaling in rice. We found that two NPR proteins in *P. patens* carry the EAR motif but that the single
386 NPR in *M. polymorpha* lacks this motif (Figure 3B and S1). The observation that the expression of
387 MpNPR or PpNPR1 in At*npr1-1* can restore the SA response suggests that bryophyte NPR proteins
388 function as SA receptors and transcriptional co-activators in *A. thaliana*, irrespective of the conservation
389 of EAR motif.

390 It is striking that mutation of the single *NPR* gene in *M. polymorpha*, Mp*NPR*, did not result in
391 diminished SA-induced transcriptional responses, although MpNPR can function as a transcriptional co-
392 activator in *A. thaliana*. Our transcriptomic analysis suggests that MpNPR functions as a transcriptional
393 co-repressor in *M. polymorpha* (Figure 4B, 4C, and S6B). In a similar fashion, the Mp*npr* mutants
394 displayed enhanced resistance against bacterial pathogens (Figure 2E–G). This is an interesting
395 observation because it implies that NPR is not important for *M. polymorpha* resistance against biotrophic
396 or hemi-biotrophic pathogens. Together with the evidence that hornworts have lost the *NPR* gene [27],

397 NPR may play a less important role in disease resistance in bryophytes. It would be instructive to
398 investigate the functions of NPR in mosses in the future, but we speculate that plants have acquired the
399 *NPR* gene during terrestrialization initially for purposes other than SA-mediated immunity. Our analyses
400 highlighted that Brassicaceae species have evolved a unique NPR repertoire. Marked changes to amino
401 acid sequence were observed to have accumulated in Brassicaceae NPR1-like proteins (Figure S1).
402 Considering the importance of AtNPR1 in SA signaling and the immune system in *A. thaliana*, this
403 finding is rather surprising. Among four Brassicaceae-specific subclades, further lineage-specific
404 expansion of NPR1 was observed (Figure S3A). This may suggest that Brassicaceae *NPR1-like* genes
405 are experiencing selective pressures. In this respect, AtNPR1 was shown to be targeted by the *P.*
406 *syringae* type III effector AvrPtoB and *Phytophthora capsici* effector RxLR48 [72,73], further
407 confirming the significance of AtNPR1 in immunity in *A. thaliana*. Effector targets are occasionally
408 integrated into NLR proteins as decoys to counteract pathogen infection [74]. Strikingly, we found that
409 one of the *Boechera stricta* NPR1 homologs, Bostr.29223s0069.1, is integrated into the C-terminus of
410 TIR-NLR (Figure S3C). Interestingly, BLASTP comparison of this TIR-NLR against the *A. thaliana*
411 database returned SNC1 (suppressor of *npr1-1*, constitutive 1) as a best hit [75]. The expression of the
412 TIR-NLR-NPR as a full-length protein needs to be confirmed, but this information seemingly suggests
413 that Brassicaceae NPR1-like proteins generally play a key role in SA-mediated immunity in
414 Brassicaceae species.

415 What then might have been the ancestral functions of NPR in the common ancestor of land
416 plants? Our transcriptomic analysis suggested potential roles of MpNPR in heat and FR signaling in *M.*
417 *polymorpha*. We indeed found that the Mp*npr* mutants display enhanced thermomorphogenesis and
418 reduced FR-induced shade avoidance (Figure 5A, 5C, and 5D). Importantly, we revealed that At*npr1-1*
419 also displays enhanced thermomorphogenesis (Figure 5B), implying that a function of NPR in
420 thermomorphogenesis is conserved in the only two sister lineages of land plants, bryophytes and
421 tracheophytes, and is thus ancient. Considering that adaptation to fluctuating temperatures was crucial
422 for plant terrestrialization, it is attractive to hypothesize that plants initially acquired *NPR* genes to deal
423 with varying abiotic components, including temperature and light quality, rather than potentially
424 detrimental microbes. In comparison with the NPR family, the BOP family seems to have undergone

425 less expansion during land plant evolution. The genome of *A. trichopoda* encodes a single *BOP* gene
426 [64], suggesting that *BOP* was not duplicated at the epsilon WGD event. In this regard, the two BOP
427 proteins encoded in the *A. thaliana* genome function redundantly [10,76,77]. Nevertheless, analyzed
428 plant species encode between zero and five copies of BOP, suggesting lineage-specific expansion and
429 loss of BOP. The function of *BOP* genes in bryophytes is not yet known, and disruption of all three *BOP*
430 genes in the moss *P. patens* did not cause any observable developmental phenotypes [78]. It is intriguing
431 that *Marchantia* liverworts have kept the *NPR* gene but lost the *BOP* gene, while *Anthoceros* hornworts
432 have lost the *NPR* gene but kept the *BOP* gene [27,33]. This may imply that *BOP* and *NPR* genes have
433 shared functions that were required for the survival of liverwort and hornwort lineages during evolution.
434 In *A. thaliana*, two BOPs have been shown to play a role in thermomorphogenesis [79], suggesting that
435 AtNPR1 and AtBOP1/2 have shared functions in thermomorphogenesis. Functional analysis of *BOP*
436 genes in hornworts and sophisticated inter-species and intra-species complementation analysis would
437 shed light on the ancestral shared functions of NPR and BOP proteins or of a hypothetical ancestral
438 protein that diverged into NPR and BOP.
439

440 **Methods**

441 **Key resources table**

Reagent or Resources	Source	Identifier
Bacterial and virus strains		
Escherichia coli DH5a	Widely distributed	N/A
Agrobacterium tumefaciens GV3101, GV2260, EHA101	Widely distributed	N/A
Pseudomonas syringae pv. *tomato* DC3000 P_{kan}:lux (*Pto*-lux)	[57]	N/A
Chemicals, peptides, and recombinant proteins		
SuperScript IV Reverse Transcriptase	ThermoFisher	Cat#18090010
In-Fusion HD cloning kit	TaKaRa	Cat#639650
NEBuilder HiFi DNA Assembly Master Mix	NEB	Cat#E2621S
LR Clonase II Plus enzyme	ThermoFisher	Cat#11791020
RNeasy Plant Mini Kit	Qiagen	Cat#74904
Experimental models: Organisms/strains		
Marchantia polymorpha: Tak-1	Takayuki Kohchi, Kyoto University	N/A
Marchantia polymorpha: Mp*npr-1*^{ge}	This study	N/A
Marchantia polymorpha: Mp*npr-2*^{ge}	This study	N/A
Marchantia polymorpha: Mp*pif*^{ko}	[80]	N/A
Marchantia polymorpha: $_{pro}$Mp*EF1α*:Mp*PIF*/Tak-1	[81]	N/A
Marchantia polymorpha: $_{pro}$Mp*NPR*:Mp*NPR*/Mp*npr-1*^{ge}	This study	N/A
Marchantia polymorpha: $_{pro}$Mp*EF1α*:Mp*NPR-mCitrine*/Tak-1	This study	N/A
Marchantia polymorpha: $_{pro}$Mp*EF1α*:At*NPR1-mCitrine*/Mp*npr-1*^{ge}	This study	N/A
Arabidopsis thaliana: Col-0	Widely distributed	N/A
Arabidopsis thaliana: *npr1-1*	[58]	N/A
Arabidopsis thaliana: *npr3-1 npr4-2*	[15]	N/A

Arabidopsis thaliana: *npr1-1 npr3-2 npr4-2*	[14]	N/A
Arabidopsis thaliana: *pif4-101*	[82]	N/A
Arabidopsis thaliana: $_{pro}$*35S:*At*NPR1-GFP/npr1-1*	[83]	N/A
Arabidopsis thaliana: $_{pro}$*35S:*Mp*NPR/npr1-1*	This study	N/A
Oligonucleotides		
Oligonucleotides used in this study can be found in Table S3	This study	N/A
Recombinant DNA		
pENTR4	ThermoFisher	Cat#A10465
pENTR4-MpNPR	This study	N/A
pENTR4-$_{pro}$*MpNPR:MpNPR*	This study	N/A
pENTR4-AtNPR1	This study	N/A
pMpGWB301	[84]	Addgene Cat#68629
pMpGWB301-$_{pro}$*MpNPR:MpNPR*	This study	N/A
pMpGWB308m	This study	N/A
pMpGWB308m-$_{pro}$*MpEF1a:MpNPR-mCitrine*	This study	N/A
pMpGWB308m-$_{pro}$*MpEF1a:AtNPR1-mCitrine*	This study	N/A
pMpGE_En01 and *pMpGE_En03*	[85]	Addgene Cat#71535
pMpGE_En01-MpNPRgRNA1	This study	N/A
pMpGE_En03-MpNPRgRNA2	This study	N/A
pMpGE010 and *pMpGE011*	[85]	Addgene Cat71536
pMpGE011-MpNPRgRNA1	This study	N/A
pMpGE010-MpNPRgRNA2	This study	N/A
pBAR-35S	Widely distributed	GenBank AJ251014.1
pBAR-35S-$_{pro}$*35S:*Mp*NPR*	This study	N/A
pMpGWB303-$_{pro}$*35S:intron-GUSPlus*	[56]	N/A
Deposited data		
Sequencing raw reads for RNA-Seq analyses	This study	BioProject PRJNA857977 and PRJNA858257
Software and algorithms		
MEGA X	[86]	https://www.megasoftware.net/
Clustal Omega	[87]	http://www.clustal.org/omega/
iTOL	[88]	https://itol.embl.de/
Omega 5.50 R4	BMG LABTECH	https://www.bmglabtech.com/microplate-reader-software/
R 4.0.4	R Core Team	https://www.r-project.org/
RStudio	RStudio Team	https://www.rstudio.com/
fastp	[89]	https://github.com/OpenGene/fastp
STAR aligner	[90]	https://github.com/alexdobin/STAR
DESeq2	[91]	https://doi.org/doi:10.18129/B9.bioc.DESeq2
PANTHER 16.0	[92]	http://www.pantherdb.org/
Prism 8	GraphPad	https://www.graphpad.com/prism

442

443 **Lead contact and materials availability**

444 Further information and requests for genetic stocks, gene constructs, resources and reagents
445 reported in this study should be directed to and will be provided by the Lead Contact, Hirofumi
446 Nakagami (nakagami@mpipz.mpg.de).

447

448 **Experimental model and subject details**

449 *Marchantia polymorpha* accession Tak-1 [93] was used as a wild type throughout this study.
450 For cultivation, gemmae were grown on half-strength Gamborg's B5 (GB5) basal media containing 1%

451 agar at 22°C under continuous white light (60 to 70 μmol m^{-2} s^{-1}). Sodium salicylate (Sigma-Aldrich)
452 was added to the media for SA-supplemented conditions to achieve desired concentrations. For far-red
453 (FR) light irradiances, gemmae were cultivated in the growth chamber (Percival Scientific), maintaining
454 continuous white light (400 to 700 nm, 65 μmol m^{-2} s^{-1}) equipped with FR LEDs (700 to 780 nm, 65
455 μmol m^{-2} s^{-1}) at 22°C. Light properties were measured by LI-250A light meter (LI-COR) equipped with
456 LI-190R quantum sensor (LI-COR) or SKR110 R/FR sensor (Skye instruments).

457 *Arabidopsis thaliana* ecotype Col-0 was used as a wild type in this study. For cultivation of *A.*
458 *thaliana*, seeds were surface-sterilized by vapor gas (Sodium hypochlorite containing 3% [v/v] HCl) for
459 4 hours and placed on half-strength Murashige and Skoog (MS) media containing 1% agar. Seeds were
460 then incubated at 4°C in the dark for 2 days before germination. Germinated seedlings were cultivated
461 at 22°C under continuous white light (60 to 70 μmol m^{-2} s^{-1}). For the SA sensitivity test, sodium
462 salicylate (Sigma-Aldrich) was added to the media to achieve desired concentrations.

463

464 **Method details**

465 *Cloning and Plasmid Construction*

466 To generate Mp*npr-1*^{ge} and *Mpnpr-2*^{ge} using CRISPR/Cas9 system, the first exon of Mp*NPR*
467 was targeted (Figure S4A). The double-strand oligonucleotides containing the target sequences were
468 synthesized and cloned into *pMpGE_En01* or *pMpGE_En03* using In-Fusion HD cloning kit (TaKaRa)
469 and BsaI restriction sites in *pMpGE_En03*, respectively. Generated entry clones were subsequently used
470 for the recombination into destination vectors *pMpGE011* and *pMpGE010* by Gateway LR clonase
471 (ThermoFisher) as manufacturer's instruction.

472 For complementation of *M. polymorpha* Mp*npr* mutants, the full-length CDS of Mp*NPR*
473 (Mp1g02380) and At*NPR1* (At1g64280) were first amplified from cDNA of *M. polymorpha* Tak-1 and
474 *A. thaliana* Col-0, respectively. For the MpNPR promoter, 5.6 kb upstream of ATG was amplified from
475 Tak-1 genomic DNA. The amplified fragments were assembled in *pENTR4* (ThermoFisher) using HiFi
476 assembly master mix (NEB), followed by recombination into *pMpGWB301* or *pMpGWB308m*
477 (modified version of *pMpGWB308* [84], replacing Citrine to mCitrine) using Gateway LR clonase
478 (ThermoFisher). For complementation of *A. thaliana* At*npr1-1* mutant, the full-length CDS of Mp*NPR*

479 was amplified from cDNA of *M. polymorpha* ecotype BoGa and cloned into *pBAR-35S* using XmaI and
480 XbaI restriction sites.
481
482 *M. polymorpha transformation*
483 The resulting constructs were transformed into *Agrobacterium tumefaciens* GV3101, GV2260
484 or EHA101 by electroporation. Subsequent transformations were carried out as described before [94].
485 Obtained transformants were grown on half-strength GB5 basal media containing 1% agar
486 supplemented with 100 μg/mL cefotaxime and 10 μg/mL hygromycin B or 0.5 μM chlorsulfuron to
487 screen non-chimeric transgenic gemmae.
488
489 *GUS histochemical assay*
490 10-day-old Mock- and 0.1 mM SA-grown *A. thaliana* seedlings were submerged in GUS
491 staining solution consisting of 0.5 mg/mL X-Gluc (5-bromo-4-chloro-3-indolyl-beta-D-glucuronic acid),
492 0.1% Triton X-100, 10 mM EDTA, 0.5 mM potassium ferricyanide, 0.5 mM potassium ferrocyanide in
493 100 mM sodium phosphate buffer (pH 7.0), followed by vacuum infiltration for 20 min. After incubation
494 in the dark at 37°C for overnight, leaves were destained by serial incubation in 30 %, 50 %, 70 % ethanol
495 for a minimum of 1 hour each before observation.
496
497 *Phylogenetic analyses*
498 Amino acid sequences of 317 homologs of MpNPR and AtBOP1 (Table S1) were aligned using
499 Clustal Omega with default parameters. To assess the reliability of a phylogenetic tree, the alignment
500 was further calculated using the Maximum Likelihood method with a bootstrap value of 1000 in MEGA
501 software [86].
502
503 *Phytohormones measurements*
504 *M. polymorpha* thalli were grown on Mock and 0.1 mM SA for 14 days before homogenization.
505 Phytohormones were extracted with methyl-tert-butyl ether (MTBE), reversed phase-separated using an
506 ACQUITY UPLC system (Waters Corp.) and analysed by nanoelectrospray ionization (nanoESI)

507 (TriVersa Nanomate, Advion BioSciences) coupled with an AB Sciex 4000 QTRAP tandem mass
508 spectrometer (AB Sciex) employed in scheduled multiple reaction monitoring modes [95]. For SA
509 measurement, the following mass transition was included 137/93 [declustering potential (DP) -25 V,
510 entrance potential (EP) -6 V, collision energy (CE) -20 V].
511
512 *Bioluminescence-based bacteria quantification*
513 Bacterial quantification in infected thallus was carried out as described before [57]. Briefly, *M.*
514 *polymorpha* were grown on autoclaved cellophane disc on half-strength GB5 media for 2 weeks. In the
515 meantime, *Pto*-lux was cultivated in King's B medium containing 30 µg/mL rifampicin to achieve 1.0
516 of OD_{600}. The saturated bacteria culture was subsequently washed and resuspended in Milli-Q water to
517 prepare bacteria suspension with 0.01 of OD_{600}. Next, 2-week-old thalli were submerged in the bacteria
518 suspension followed by vacuum for 5 min and incubated for 0 to 3 days on humid filter papers. After
519 incubation, thallus discs (5 mm diameter) were punched from the basal and apical region using a sterile
520 biopsy punch (pfm medical) and transferred to a 96-well plate (VWR). The bioluminescence was
521 measured in the FLUOstar Omega plate reader (BMG Labtech).
522
523 *Agrobacterium-mediated transient transformation*
524 Transient transformation was carried out as described before [56]. A single colony of
525 *Agrobacterium tumefaciens* strain GV3101::pMP90 harboring $_{pro}$*35S:intron-GUSPlus* was inoculated
526 into Luria-Bertani medium containing spectinomycin antibiotics and cultured for 2 days at 28°C.
527 Bacterial cells were collected from 1 ml culture by centrifugation, suspended in 5 ml of 0M51C medium
528 [96,97] containing 2% sucrose and 100 µM 3,5-dimethoxy-4-hydroxyacetophenone (acetosyringone)
529 and cultured for 5 hours at 28 °C. In parallel, Tak-1 and Mp*npr-1*^{ge} gemmae were cultured on the agar
530 plates for 14 days at 22 °C under continuous light. The bacterial culture was diluted with 0M51C
531 medium containing 2 % sucrose and 100 µM acetosyringone to be at 0.02 of OD600, and then thalli
532 were transferred into the 50 ml bacterial suspension. The thalli and *Agrobacterium* were co-cultured at
533 22 °C under continuous light for 3 days with shaking (120 rpm).
534

535 *RNA-Seq and data analysis*

536 Total RNA was isolated from 2-week-old *M. polymorpha* Tak-1 and Mp*npr-1*^{ge} treated with
537 Mock or 1 mM SA for 2, 6, and 12 hours. For RNA-Seq analysis of 7-day-old gemmae grown in liquid
538 half-strength GB5 medium with 0.1% (w/v) sucrose at 22 °C under continuous light with shaking (120
539 rpm), total RNA was isolated from *M. polymorpha* Tak-1 and Mp*npr-1*^{ge} gemmae treated with Mock
540 (water), 1 mM SA, Mock (DMSO), and 0.5 mM BTH for 24 hours. Library preparation and sequencing
541 were performed by the Max Planck-Genome-center, Cologne (https://mpgc.mpipz.mpg.de), on the
542 Illumina HiSeq 3000 platform. Raw reads were processed by fastp [89] for quality control and trimming.
543 The *M. polymorpha* genomes and gene annotations (MpTak_v6.1) [98] were used for mapping reads
544 and counting transcripts per gene in STAR aligner [90]. The genes with less than the average of 10 read
545 counts were excluded, and the log2 fold difference of the gene expression between conditions was
546 calculated in R package DESeq2 [91]. Genes with statistical significance (FDR adjusted p-value < 0.05)
547 were selected for further analyses.

548

549 **Quantification and statistical analysis**

550 Statistical details, including sample numbers, error bars, and p-value cut-offs, were shown in
551 corresponding figure legends. Unless otherwise specified, all statistical significances were calculated
552 using the R function pairwise.t.test with pooled SD. The Benjamini–Hochberg method was then used
553 for correcting the multiple hypothesis testing. Linear regression and calculation of correlation
554 coefficients were performed using the R function lm and cor, respectively.

555

556 **Data availability**

557 Sequencing raw reads used in transcriptomic analyses in this study have been deposited under the
558 accession BioProject PRJNA857977 and PRJNA858257.

559

560 **Acknowledgements**

561 The authors are grateful to Takayuki Kohchi (Kyoto University, Japan) for providing pMpGWB and
562 pMpGE vectors and Mp*pif*^{ko} and $_{pro}$Mp*EF1α:*Mp*PIF*/Tak-1 plants, Yuelin Zhang (The University of

British Columbia, Canada) for providing At*npr1-1*, At*npr3-2 npr4-2*, and At*npr1-1 npr3-2 npr4-2* seeds, George Coupland (MPIPZ, Germany) for providing At*pif4* seeds, and Sabine Freitag (University of Göttingen, Germany) for expert technical assistance. We thank Neysan Donnelly (MPIPZ, Germany) for editing the manuscript.

Author contributions

H.-W.J., H.I., and H.N. designed the research. H.I. performed phylogenetic and alignment analysis. H.I., S.N., and J.K. generated Mp*npr* mutants. H.-W.J. and H.I. generated Mp*npr-1*^{ge} complementation and MpNPR overexpression lines. N.G. and S.Z. generated At*npr1-1* complementation lines. H.-W.J. and H.I. performed SA and BTH sensitivity assays. C.H. and I.F. quantified phytohormones. H.-W.J. and T.S. performed bioluminescence-based bacteria quantification. H.I. performed transient transformation assay. H.-W.J., H.I., and S.M. performed transcriptomic analyses. H.-W.J. performed all other experiments. H.-W.J., H.I., and H.N. wrote the manuscript. All authors corrected the manuscript.

Funding

This project was supported by the Max Planck Society. We are grateful for funding by the Deutsche Forschungsgemeinschaft (DFG) to I.F. (INST 186/822-1), N.G. (GU 1839/1-2), and S.Z. (SZ 259/11).

Figure legends

Figure 1. Phylogenetic analysis and amino acid conservation of 194 NPR and 123 BOP proteins from 68 plant species.

(A) Unrooted phylogenetic tree showing that 194 NPR proteins were clustered into four major clades; angiosperms NPR1/2, angiosperms NPR3/4, non-seed plants NPR, and gymnosperms NPR clades. Brassicaceae NPR1- to 4-like subclades were further clustered into angiosperm NPR clades. (B–D) Conservation of functional amino acids and motifs associated with the molecular functions of AtNPR1. Cysteines required for AtNPR1 accumulation and oligomerization (B), Arg432 responsible for SA binding in AtNPR1 (C), and the EAR motif (DLNxxP) responsible for transcriptional co-repression activity (D) are shown.

591

592 **Figure 2. Phenotypic analyses of Mp*npr* mutants in SA and SA-induced immune responses.**

593 (A, B) SA hypersensitivity in the growth of Mp*npr-1*^{ge} and Mp*npr-2*^{ge} compared to Tak-1. Scale bar, 1
594 cm (n = 8). (C, D) SA and jasmonate measurements in Tak-1 and Mp*npr* mutants grown on mock and
595 SA-supplemented conditions (n = 5). (E) Quantification of bacterial growth in the basal and apical
596 thallus, inoculated with the bioluminescent *Pto*-lux (n = 8). DPI, days post-inoculation. (F–G) Transient
597 transformation of Tak-1 and Mp*npr-1*^{ge} using *Agrobacterium* carrying *intron-GUSPlus* (n = 6). (B–E,
598 G) Different letters represent statistical significances (Tukey's test; $p < 0.01$). Error bars indicate SD.

599

600 **Figure 3. Inter-species complementation analysis in *M. polymorpha* and *A. thaliana*.**

601 (A, B) Complementation of SA hypersensitivity in Mp*npr-1*^{ge} by introducing $_{pro}$Mp*NPR:*Mp*NPR* and
602 $_{pro}$Mp*EF1a:*At*NPR1-mCitrine*. Scale bar, 1 cm (n = 8). (C) Complementation of SA hypersensitivity in
603 At*npr1-1* by expression of $_{pro}$*35S:*Mp*NPR* (n = 3). (D) GUS staining results showed that Mp*NPR*
604 overexpression restored SA-induced *BGL2::GUS* expression in At*npr1-1*. Scale bars, 1 mm. (B, C)
605 Different letters represent statistically significant differences (Tukey's test; $p < 0.01$). Error bars indicate
606 SD.

607

608 **Figure 4. RNA-Seq analysis comparing SA-induced transcriptional reprogramming in Tak-1 and**
609 **Mp*npr-1*^{ge}.**

610 (A) Heatmap of 425 SA-induced DEGs ($|\log2FC| \geq 1$, adjusted $p < 0.05$, 6 hpi) identified in Tak-1 and
611 correlated genes in Mp*npr-1*^{ge}. (B) Number of SA-induced DEGs ($|\log2FC| \geq 1$, adjusted $p < 0.05$) in
612 Tak-1 and Mp*npr-1*^{ge} for 2, 6, and 12 hpi. (C, D) GO enrichment analyses using SA-induced DEGs in
613 Tak-1 (C) and Mp*npr-1*^{ge} (D). Top 10 GO terms beginning with 'response to' are shown (FDR < 0.001).
614 (E) Venn diagram showing numbers of DEGs induced by Mp*npr-1*^{ge} in each treatment ($|\log2FC| \geq 1$,
615 adjusted $p < 0.05$, 6 hpi). (F) Heatmap of 143 DEGs identified in E, showing MpNPR-dependent and
616 SA-irresponsive DEGs except for 20 genes (arrowhead). (G) GO enrichment analysis using 123 DEGs
617 identified in F.

618

619 **Figure 5. Putative roles of MpNPR in thermomorphogenesis and shade avoidance syndrome in *M.***

620 ***polymorpha*.**

621 (A) Enhanced thermomorphogenesis in Mp*npr* mutants compared to Tak-1 at 30 °C. Twenty-day-old

622 thalli are shown. Scale bar, 1 cm. (B) Hypocotyl length of At*npr* mutants grown at 22 and 28 °C for 6

623 days (n ≥ 6). (C) Representative pictures of *M. polymorpha* thalli viewed from the side. Scale bar, 0.5

624 cm. (D) Thallus elevation angles quantified from 2-week-old *M. polymorpha* grown with or without far-

625 red light (n = 9). Different letters represent statistically significant differences (Tukey's test; $p < 0.01$).

626 Error bars indicate SD.

627

628 **Supplemental information**

629 **Figure S1** Phylogenetic tree showing the conservations of functional residues and motifs of 194

630 NPR proteins, related to Figure 1

631 **Figure S2** The exon-intron organization in the BTB/POZ-encoding regions are highly conserved

632 between NPR and BOP families

633 **Figure S3** Gene duplications in Brassicaceae-specific NPR subclades and integration of *Boechera*

634 *stricta* NPR1 homolog into TIR-NLR protein, related to Figure 1A

635 **Figure S4** Generation of Mp*npr* mutants using CRISPR/Cas9 system and complementation of the

636 SA-hypersensitivity phenotype in the mutants

637 **Figure S5** BTH sensitivity was unchanged in Mp*npr* mutants compared to Tak-1

638 **Figure S6** RNA-Seq analysis comparing Tak-1 and Mp*npr-1*^{ge} thalli in Mock and SA conditions

639 **Figure S7** RNA-Seq analysis comparing Tak-1 and Mp*npr-1*^{ge} gemmae in Mock, SA, and BTH

640 conditions

641 **Table S1** NPR and BOP homologs used for phylogenetic analysis

642 **Table S2** Reference genomes of species used in BLASTP

643 **Table S3** Oligonucleotides used in this study

644

645 **References**

646 1. Peng, Y., Yang, J., Li, X., and Zhang, Y. (2021). Salicylic Acid: Biosynthesis and Signaling.
647 Annual Review of Plant Biology *72*, 761–791.

648 2. Zhou, J., and Zhang, Y. (2020). Plant Immunity: Danger Perception and Signaling. Cell *181*,
649 978–989.

650 3. Blanco, F., Salinas, P., Cecchini, N.M., Jordana, X., Van Hummelen, P., Alvarez, M.E., and
651 Holuigue, L. (2009). Early genomic responses to salicylic acid in Arabidopsis. Plant Molecular
652 Biology *70*, 79–102.

653 4. Wang, D., Amornsiripanitch, N., and Dong, X. (2006). A Genomic Approach to Identify
654 Regulatory Nodes in the Transcriptional Network of Systemic Acquired Resistance in Plants.
655 PLoS Pathogens *2*, e123.

656 5. Xu, G., Yuan, M., Ai, C., Liu, L., Zhuang, E., Karapetyan, S., Wang, S., and Dong, X. (2017).
657 UORF-mediated translation allows engineered plant disease resistance without fitness costs.
658 Nature *545*, 491–494.

659 6. Aravind, L., and Koonin, E. v. (1999). Fold prediction and evolutionary analysis of the POZ
660 domain: structural and evolutionary relationship with the potassium channel tetramerization
661 domain. Journal of Molecular Biology *285*, 1353–1361.

662 7. Cao, H., Glazebrook, J., Clarke, J.D., Volko, S., and Dong, X. (1997). The Arabidopsis NPR1
663 Gene That Controls Systemic Acquired Resistance Encodes a Novel Protein Containing
664 Ankyrin Repeats. Cell *88*, 57–63.

665 8. Li, J., Mahajan, A., and Tsai, M.-D. (2006). Ankyrin Repeat: A Unique Motif Mediating
666 Protein−Protein Interactions. Biochemistry *45*, 15168–15178.

667 9. Ryals, J., Weymann, K., Lawton, K., Friedrich, L., Ellis, D., Steiner, H.Y., Johnson, J.,
668 Delaney, T.P., Jesse, T., Vos, P., et al. (1997). The Arabidopsis NIM1 protein shows homology
669 to the mammalian transcription factor inhibitor I kappa B. The Plant Cell *9*, 425–439.

670 10. Hepworth, S.R., Zhang, Y., McKim, S., Li, X., and Haughn, G.W. (2005). BLADE-ON-
671 PETIOLE–Dependent Signaling Controls Leaf and Floral Patterning in Arabidopsis. The Plant
672 Cell *17*, 1434–1448.

673 11. Ha, C.M., Jun, J.H., Nam, H.G., and Fletcher, J.C. (2004). BLADE-ON-PETIOLE1 Encodes a
674 BTB/POZ Domain Protein Required for Leaf Morphogenesis in *Arabidopsis thaliana*. Plant
675 and Cell Physiology *45*, 1361–1370.

676 12. Ha, C.M., Ji, H.J., Hong, G.N., and Fletcher, J.C. (2007). BLADE-ON-PETIOLE1 and 2
677 control Arabidopsis lateral organ fate through regulation of LOB domain and adaxial-abaxial
678 polarity genes. The Plant Cell *19*, 1809–1825.

679 13. Castelló, M.J., Medina-Puche, L., Lamilla, J., and Tornero, P. (2018). NPR1 paralogs of
680 Arabidopsis and their role in salicylic acid perception. PLoS ONE *13*, 1–20.

681 14. Ding, Y., Sun, T., Ao, K., Peng, Y., Zhang, Y., Li, X., and Zhang, Y. (2018). Opposite Roles of
682 Salicylic Acid Receptors NPR1 and NPR3/NPR4 in Transcriptional Regulation of Plant
683 Immunity. Cell *173*, 1454-1467.e15.

684 15. Zhang, Y., Cheng, Y.T., Qu, N., Zhao, Q., Bi, D., and Li, X. (2006). Negative regulation of
685 defense responses in Arabidopsis by two NPR1 paralogs. Plant Journal *48*, 647–656.

686 16. Fu, Z.Q., Yan, S., Saleh, A., Wang, W., Ruble, J., Oka, N., Mohan, R., Spoel, S.H., Tada, Y.,
687 Zheng, N., et al. (2012). NPR3 and NPR4 are receptors for the immune signal salicylic acid in
688 plants. Nature *486*, 228–232.

689 17. Wu, Y., Zhang, D., Chu, J.Y., Boyle, P., Wang, Y., Brindle, I.D., De Luca, V., and Després, C.
690 (2012). The Arabidopsis NPR1 Protein Is a Receptor for the Plant Defense Hormone Salicylic
691 Acid. Cell Reports *1*, 639–647.

692 18. Shimizu, K., Suzuki, H., Uemura, T., Nozawa, A., Desaki, Y., Hoshino, R., Yoshida, A., Abe,
693 H., Nishiyama, M., Nishiyama, C., et al. (2022). Immune gene activation by NPR and TGA
694 transcriptional regulators in the model monocot *Brachypodium distachyon*. The Plant Journal
695 *110*, 470–481.

696 19. Ohta, M., Matsui, K., Hiratsu, K., Shinshi, H., and Ohme-Takagi, M. (2001). Repression
697 Domains of Class II ERF Transcriptional Repressors Share an Essential Motif for Active
698 Repression. The Plant Cell *13*, 1959.

699 20. Kumar, S., Zavaliev, R., Wu, Q., Zhou, Y., Cheng, J., Dillard, L., Powers, J., Withers, J., Zhao,
700 J., Guan, Z., et al. (2022). Structural basis of NPR1 in activating plant immunity. Nature *605*,
701 561–566.

702 21. Withers, J., and Dong, X. (2016). Posttranslational Modifications of NPR1: A Single Protein
703 Playing Multiple Roles in Plant Immunity and Physiology. PLoS Pathogens *12*, 1–9.

704 22. Mou, Z., Fan, W., and Dong, X. (2003). Inducers of Plant Systemic Acquired Resistance
705 Regulate NPR1 Function through Redox Changes. Cell *113*, 935–944.

706 23. Tada, Y., Spoel, S.H., Pajerowska-Mukhtar, K., Mou, Z., Song, J., Wang, C., Zuo, J., and
707 Dong, X. (2008). Plant Immunity Requires Conformational Charges of NPR1 via S-
708 Nitrosylation and Thioredoxins. Science (1979) *321*, 952–956.

709 24. Ishihama, N., Choi, S., Noutoshi, Y., Saska, I., Asai, S., Takizawa, K., He, S.Y., Osada, H.,
710 Shirasu, K., and Takizawa, K. (2021). Oxicam-type non-steroidal anti-inflammatory drugs
711 inhibit NPR1-mediated salicylic acid pathway. Nature Communications *12*, 7303.

712 25. Zavaliev, R., Mohan, R., Chen, T., and Dong, X. (2020). Formation of NPR1 Condensates
713 Promotes Cell Survival during the Plant Immune Response. Cell *119*, 1–16.

714 26. Leebens-Mack, J.H., Barker, M.S., Carpenter, E.J., Deyholos, M.K., Gitzendanner, M.A.,
715 Graham, S.W., Grosse, I., Li, Z., Melkonian, M., Mirarab, S., et al. (2019). One thousand plant
716 transcriptomes and the phylogenomics of green plants. Nature *574*, 679–685.

717 27. Li, F.-W., Nishiyama, T., Waller, M., Frangedakis, E., Keller, J., Li, Z., Fernandez-Pozo, N.,
718 Barker, M.S., Bennett, T., Blázquez, M.A., et al. (2020). Anthoceros genomes illuminate the
719 origin of land plants and the unique biology of hornworts. Nature Plants *6*, 259–272.

720 28. Puttick, M.N., Morris, J.L., Williams, T.A., Cox, C.J., Edwards, D., Kenrick, P., Pressel, S.,
721 Wellman, C.H., Schneider, H., Pisani, D., et al. (2018). The Interrelationships of Land Plants
722 and the Nature of the Ancestral Embryophyte. Current Biology *28*, 733-745.e2.

723 29. Bowman, J.L., Araki, T., and Kohchi, T. (2016). Marchantia : Past, Present and Future. Plant
724 and Cell Physiology *57*, 205–209.

725 30. Strother, P.K., and Taylor, W.A. (2018). The Evolutionary Origin of the Plant Spore in
726 Relation to the Antithetic Origin of the Plant Sporophyte. In Transformative Paleobotany:
727 Papers to Commemorate the Life and Legacy of Thomas N. Taylor, M. Krings, C. J. Harper, N.
728 R. Cúneo, and G. W. Rothwell, eds. (Elsevier), pp. 3–20.

729 31. Naramoto, S., Hata, Y., Fujita, T., and Kyozuka, J. (2022). The bryophytes *Physcomitrium*
730 *patens* and *Marchantia polymorpha* as model systems for studying evolutionary cell and
731 developmental biology in plants. The Plant Cell *34*, 228–246.

732 32. Wickett, N.J., Mirarab, S., Nguyen, N., Warnow, T., Carpenter, E., Matasci, N.,
733 Ayyampalayam, S., Barker, M.S., Burleigh, J.G., Gitzendanner, M.A., et al. (2014).
734 Phylotranscriptomic analysis of the origin and early diversification of land plants. Proceedings
735 of the National Academy of Sciences *111*, E4859–E4868.

736 33. Bowman, J.L., Kohchi, T., Yamato, K.T., Jenkins, J., Shu, S., Ishizaki, K., Yamaoka, S.,
737 Nishihama, R., Nakamura, Y., Berger, F., et al. (2017). Insights into Land Plant Evolution
738 Garnered from the *Marchantia polymorpha* Genome. Cell *171*, 287-304.e15.

739 34. Lang, D., Ullrich, K.K., Murat, F., Fuchs, J., Jenkins, J., Haas, F.B., Piednoel, M., Gundlach,
740 H., van Bel, M., Meyberg, R., et al. (2018). The *Physcomitrella patens* chromosome-scale
741 assembly reveals moss genome structure and evolution. The Plant Journal *93*, 515–533.

742 35. Peng, Y., Sun, T., and Zhang, Y. (2017). Perception of Salicylic Acid in *Physcomitrella patens*.
743 Frontiers in Plant Science *8*, 2145.

744 36. Backer, R., Naidoo, S., and van den Berg, N. (2019). The NONEXPRESSOR OF
745 PATHOGENESIS-RELATED GENES 1 (NPR1) and related family: Mechanistic insights in
746 plant disease resistance. Frontiers in Plant Science *10*, 1–21.

747 37. Gao, C.S., Kou, X.J., Li, H.P., Zhang, J.B., Saad, A.S.I., and Liao, Y.C. (2013). Inverse effects
748 of Arabidopsis NPR1 gene on fusarium seedling blight and fusarium head blight in transgenic
749 wheat. Plant Pathology *62*, 383–392.

750 38. Kumar, V., Joshi, S.G., Bell, A.A., and Rathore, K.S. (2013). Enhanced resistance against
751 *Thielaviopsis basicola* in transgenic cotton plants expressing Arabidopsis NPR1 gene.
752 Transgenic Research *22*, 359–368.

753 39. Lin, W.-C., Lu, C.-F., Wu, J.-W., Cheng, M.-L., Lin, Y.-M., Yang, N.-S., Black, L., Green,
754 S.K., Wang, J.-F., and Cheng, C.-P. (2004). Transgenic tomato plants expressing the
755 Arabidopsis NPR1 gene display enhanced resistance to a spectrum of fungal and bacterial
756 diseases. Transgenic Research *13*, 567–581.

757 40. Makandar, R., Essig, J.S., Schapaugh, M.A., Trick, H.N., and Shah, J. (2006). Genetically
758 Engineered Resistance to Fusarium Head Blight in Wheat by Expression of Arabidopsis NPR1.
759 Molecular Plant-Microbe Interactions® *19*, 123–129.

760 41. Matthews, B.F., Beard, H., Brewer, E., Kabir, S., MacDonald, M.H., and Youssef, R.M.
761 (2014). Arabidopsis genes, AtNPR1, AtTGA2 and AtPR-5, confer partial resistance to soybean
762 cyst nematode (*Heterodera glycines*) when overexpressed in transgenic soybean roots. BMC
763 Plant Biology *14*, 96.

764 42. Parkhi, V., Kumar, V., Campbell, L.A.M., Bell, A.A., Shah, J., and Rathore, K.S. (2010).
765 Resistance against various fungal pathogens and reniform nematode in transgenic cotton plants
766 expressing Arabidopsis NPR1. Transgenic Research *19*, 959–975.

767 43. Parkhi, V., Kumar, V., Campbell, L.A.M., Bell, A.A., Rathore, K.S., Campbell, Bell, and
768 Rathore, K.S. (2010). Expression of Arabidopsis NPR1 in Transgenic Cotton Confers
769 Resistance to Non-defoliating Isolates of *Verticillium dahliae* but not the Defoliating Isolates.
770 Journal of Phytopathology *158*, 822–825.

771 44. Potlakayala, S.D., DeLong, C., Sharpe, A., and Fobert, P.R. (2007). Conservation of NON-
772 EXPRESSOR OF PATHOGENESIS-RELATED GENES1 function between *Arabidopsis*
773 *thaliana* and *Brassica napus*. Physiological and Molecular Plant Pathology *71*, 174–183.

774 45. Wally, O., Jayaraj, J., and Punja, Z.K. (2009). Broad-spectrum disease resistance to
775 necrotrophic and biotrophic pathogens in transgenic carrots (*Daucus carota* L.) expressing an
776 Arabidopsis NPR1 gene. Planta *231*, 131–141.

777 46. Sugano, S., Jiang, C.J., Miyazawa, S.I., Masumoto, C., Yazawa, K., Hayashi, N., Shimono, M.,
778 Nakayama, A., Miyao, M., and Takatsuji, H. (2010). Role of OsNPR1 in rice defense program
779 as revealed by genome-wide expression analysis. Plant Molecular Biology *74*, 549–562.

780 47. Olate, E., Jiménez-Gómez, J.M., Holuigue, L., and Salinas, J. (2018). NPR1 mediates a novel
781 regulatory pathway in cold acclimation by interacting with HSFA1 factors. Nature Plants *4*,
782 811–823.

783 48. Lai, Y.-S., Renna, L., Yarema, J., Ruberti, C., He, S.Y., and Brandizzi, F. (2018). Salicylic
784 acid-independent role of NPR1 is required for protection from proteotoxic stress in the plant
785 endoplasmic reticulum. Proceedings of the National Academy of Sciences *115*, E5203–E5212.

786 49. Rochon, A., Boyle, P., Wignes, T., Fobert, P.R., and Després, C. (2006). The coactivator
787 function of Arabidopsis NPR1 requires the core of its BTB/POZ domain and the oxidation of
788 C-terminal cysteines. The Plant Cell *18*, 3670–3685.

789 50. Innes, R. (2018). The Positives and Negatives of NPR: A Unifying Model for Salicylic Acid
790 Signaling in Plants. Cell *173*, 1314–1315.

791 51. Gimenez-Ibanez, S., Zamarreño, A.M., García-Mina, J.M., and Solano, R. (2019). An
792 Evolutionarily Ancient Immune System Governs the Interactions between *Pseudomonas*
793 *syringae* and an Early-Diverging Land Plant Lineage. Current Biology *29*, 2270-2281.e4.

794 52. Zhang, X., Chen, S., and Mou, Z. (2010). Nuclear localization of NPR1 is required for
795 regulation of salicylate tolerance, isochorismate synthase 1 expression and salicylate
796 accumulation in Arabidopsis. Journal of Plant Physiology *167*, 144–148.

797 53. Matsui, H., Iwakawa, H., Hyon, G.-S., Yotsui, I., Katou, S., Monte, I., Nishihama, R., Franzen,
798 R., Solano, R., and Nakagami, H. (2020). Isolation of Natural Fungal Pathogens from
799 *Marchantia polymorpha* Reveals Antagonism between Salicylic Acid and Jasmonate during
800 Liverwort–Fungus Interactions. Plant and Cell Physiology *61*, 265–275.

801 54. Monte, I., Ishida, S., Zamarreño, A.M., Hamberg, M., Franco-Zorrilla, J.M., García-Casado,
802 G., Gouhier-Darimont, C., Reymond, P., Takahashi, K., García-Mina, J.M., et al. (2018).
803 Ligand-receptor co-evolution shaped the jasmonate pathway in land plants. Nature Chemical
804 Biology *14*, 480–488.

805 55. Roetschi, A., Si-Ammour, A., Belbahri, L., Mauch, F., and Mauch-Mani, B. (2001).
806 Characterization of an Arabidopsis-Phytophthora Pathosystem: resistance requires a functional
807 PAD2 gene and is independent of salicylic acid, ethylene and jasmonic acid signalling. The
808 Plant Journal *28*, 293–305.

809 56. Iwakawa, H., Melkonian, K., Schlüter, T., Jeon, H.-W., Nishihama, R., Motose, H., and
810 Nakagami, H. (2021). *Agrobacterium*-Mediated Transient Transformation of Marchantia
811 Liverworts. Plant and Cell Physiology *62*, 1718–1727.

812 57. Matsumoto, A., Schlüter, T., Melkonian, K., Takeda, A., Nakagami, H., and Mine, A. (2022).
813 A versatile Tn7 transposon-based bioluminescence tagging tool for quantitative and spatial
814 detection of bacteria in plants. Plant Communications *3*, 100227.

815 58. Cao, H., Bowling, S.A., Gordon, A.S., and Dong, X. (1994). Characterization of an
816 Arabidopsis Mutant That Is Nonresponsive to Inducers of Systemic Acquired Resistance. The
817 Plant Cell *6*, 1583.

818 59. Carella, P., Gogleva, A., Hoey, D.J., Bridgen, A.J., Stolze, S.C., Nakagami, H., and Schornack,
819 S. (2019). Conserved Biochemical Defenses Underpin Host Responses to Oomycete Infection
820 in an Early-Divergent Land Plant Lineage. Current Biology *29*, 2282-2294.e5.

821 60. Ludwig, W., Hayes, S., Trenner, J., Delker, C., and Quint, M. (2021). On the evolution of plant
822 thermomorphogenesis. Journal of Experimental Botany *72*, 7345–7358.

823 61. Casal, J.J., Sanchez, R.A., and Deregibus, V.A. (1986). The effect of plant density on tillering:
824 The involvement of R/FR ratio and the proportion of radiation intercepted per plant.
825 Environmental and Experimental Botany *26*, 365–371.

826 62. Franklin, K.A., and Whitelam, G.C. (2005). Phytochromes and Shade-avoidance Responses in
827 Plants. Annals of Botany *96*, 169–175.

828 63. Ballaré, C.L. (1999). Keeping up with the neighbours: phytochrome sensing and other
829 signalling mechanisms. Trends in Plant Science *4*, 97–102.

830 64. Albert, V.A., Barbazuk, W.B., DePamphilis, C.W., Der, J.P., Leebens-Mack, J., Ma, H.,
831 Palmer, J.D., Rounsley, S., Sankoff, D., Schuster, S.C., et al. (2013). The Amborella Genome
832 and the Evolution of Flowering Plants. Science (1979) *342*.

833 65. Franzke, A., Lysak, M.A., Al-Shehbaz, I.A., Koch, M.A., and Mummenhoff, K. (2011).
834 Cabbage family affairs: the evolutionary history of Brassicaceae. Trends in Plant Science *16*,
835 108–116.

836 66. Ren, R., Wang, H., Guo, C., Zhang, N., Zeng, L., Chen, Y., Ma, H., and Qi, J. (2018).
837 Widespread Whole Genome Duplications Contribute to Genome Complexity and Species
838 Diversity in Angiosperms. Molecular Plant *11*, 414–428.

839 67. Yuan, Y., Zhong, S., Li, Q.Q., Zhu, Z., Lou, Y., Wang, L., Wang, J., Wang, M., Li, Q.Q.,
840 Yang, D., et al. (2007). Functional analysis of rice NPR1-like genes reveals that OsNPR1/NH1
841 is the rice orthologue conferring disease resistance with enhanced herbivore susceptibility.
842 Plant Biotechnology Journal *5*, 313–324.

843 68. Fister, A.S., Landherr, L., Maximova, S.N., and Guiltinan, M.J. (2018). Transient Expression
844 of CRISPR/Cas9 Machinery Targeting TcNPR3 Enhances Defense Response in *Theobroma*
845 *cacao*. Frontiers in Plant Science *9*, 1–15.

846 69. Shi, Z., Zhang, Y., Maximova, S.N., and Guiltinan, M.J. (2013). TcNPR3 from *Theobroma*
847 *cacao* functions as a repressor of the pathogen defense response. BMC Plant Biology *13*, 1–12.

848 70. Zhang, Y., Shi, J., Liu, J.-Y., Zhang, Y., Zhang, J.-D., and Guo, X.-Q. (2010). Identification of
849 a novel NPR1-like gene from *Nicotiana glutinosa* and its role in resistance to fungal, bacterial
850 and viral pathogens. Plant Biology *12*, 23–34.

851 71. Shi, Z., Maximova, S.N., Liu, Y., Verica, J., and Guiltinan, M.J. (2010). Functional analysis of
852 the *Theobroma cacao* NPR1 gene in Arabidopsis. BMC Plant Biology *10*, 248.

853 72. Chen, H., Chen, J., Li, M., Chang, M., Xu, K., Shang, Z., Zhao, Y., Palmer, I., Zhang, Y.,
854 McGill, J., et al. (2017). A Bacterial Type III Effector Targets the Master Regulator of Salicylic
855 Acid Signaling, NPR1, to Subvert Plant Immunity. Cell Host and Microbe *22*, 777-788.e7.

856 73. Li, Q., Chen, Y., Wang, J., Zou, F., Jia, Y., Shen, D., Zhang, Q., Jing, M., Dou, D., and Zhang,
857 M. (2019). A *Phytophthora capsici* virulence effector associates with NPR1 and suppresses
858 plant immune responses. Phytopathology Research *1*, 6.

859 74. Sarris, P.F., Cevik, V., Dagdas, G., Jones, J.D.G., and Krasileva, K. V. (2016). Comparative
860 analysis of plant immune receptor architectures uncovers host proteins likely targeted by
861 pathogens. BMC Biology *14*, 8.

862 75. Zhang, Y., Goritschnig, S., Dong, X., and Li, X. (2003). A Gain-of-Function Mutation in a
863 Plant Disease Resistance Gene Leads to Constitutive Activation of Downstream Signal
864 Transduction Pathways in *suppressor of npr1-1 , constitutive 1*. The Plant Cell *15*, 2636–2646.

865 76. Norberg, M., Holmlund, M., and Nilsson, O. (2005). The BLADE ON PETIOLE genes act
866 redundantly to control the growth and development of lateral organs. Development *132*, 2203–
867 2213.

868 77. Xu, M., Hu, T., McKim, S.M., Murmu, J., Haughn, G.W., and Hepworth, S.R. (2010).
869 Arabidopsis BLADE-ON-PETIOLE1 and 2 promote floral meristem fate and determinacy in a
870 previously undefined pathway targeting APETALA1 and AGAMOUS-LIKE24. The Plant
871 Journal *63*, 974–989.

872 78. Hata, Y., Naramoto, S., and Kyozuka, J. (2019). BLADE-ON-PETIOLE genes are not involved
873 in the transition from protonema to gametophore in the moss *Physcomitrella patens*. Journal of
874 Plant Research *132*, 617–627.

875 79. Zhang, B., Holmlund, M., Lorrain, S., Norberg, M., Bakó, L.S., Fankhauser, C., and Nilsson,
876 O. (2017). BLADE-ON-PETIOLE proteins act in an E3 ubiquitin ligase complex to regulate
877 PHYTOCHROME INTERACTING FACTOR 4 abundance. Elife *6*, 1–19.

878 80. Inoue, K., Nishihama, R., Kataoka, H., Hosaka, M., Manabe, R., Nomoto, M., Tada, Y.,
879 Ishizaki, K., and Kohchi, T. (2016). Phytochrome signaling is mediated by PHYTOCHROME
880 INTERACTING FACTOR in the liverwort Marchantia polymorpha. The Plant Cell *28*, 1406–
881 1421.

882 81. Inoue, K., Nishihama, R., Araki, T., and Kohchi, T. (2019). Reproductive Induction is a Far-
883 Red High Irradiance Response that is Mediated by Phytochrome and PHYTOCHROME
884 INTERACTING FACTOR in *Marchantia polymorpha*. Plant and Cell Physiology *60*, 1136–
885 1145.

886 82. Lorrain, S., Allen, T., Duek, P.D., Whitelam, G.C., and Fankhauser, C. (2007). Phytochrome-
887 mediated inhibition of shade avoidance involves degradation of growth-promoting bHLH
888 transcription factors. The Plant Journal *53*, 312–323.

889 83. Lindermayr, C., Sell, S., Müller, B., Leister, D., and Durner, J. (2010). Redox Regulation of the
890 NPR1-TGA1 System of *Arabidopsis thaliana* by Nitric Oxide. The Plant Cell *22*, 2894–2907.

891 84. Ishizaki, K., Nishihama, R., Ueda, M., Inoue, K., Ishida, S., Nishimura, Y., Shikanai, T., and
892 Kohchi, T. (2015). Development of Gateway Binary Vector Series with Four Different
893 Selection Markers for the Liverwort *Marchantia polymorpha*. PLOS ONE *10*, e0138876.

894 85. Sugano, S.S., Nishihama, R., Shirakawa, M., Takagi, J., Matsuda, Y., Ishida, S., Shimada, T.,
895 Hara-Nishimura, I., Osakabe, K., and Kohchi, T. (2018). Efficient CRISPR/Cas9-based
896 genome editing and its application to conditional genetic analysis in *Marchantia polymorpha*.
897 PLoS ONE *13*, 1–22.

898 86. Kumar, S., Stecher, G., Li, M., Knyaz, C., and Tamura, K. (2018). MEGA X: Molecular
899 evolutionary genetics analysis across computing platforms. Molecular Biology and Evolution
900 *35*, 1547–1549.

901 87. Sievers, F., Wilm, A., Dineen, D., Gibson, T.J., Karplus, K., Li, W., Lopez, R., McWilliam, H.,
902 Remmert, M., Söding, J., et al. (2011). Fast, scalable generation of high-quality protein
903 multiple sequence alignments using Clustal Omega. Molecular Systems Biology *7*, 539.

904 88. Letunic, I., and Bork, P. (2021). Interactive Tree Of Life (iTOL) v5: an online tool for
905 phylogenetic tree display and annotation. Nucleic Acids Research *49*, W293–W296.

906 89. Chen, S., Zhou, Y., Chen, Y., and Gu, J. (2018). Fastp: An ultra-fast all-in-one FASTQ
907 preprocessor. Bioinformatics *34*, i884–i890.

908 90. Dobin, A., Davis, C.A., Schlesinger, F., Drenkow, J., Zaleski, C., Jha, S., Batut, P., Chaisson,
909 M., and Gingeras, T.R. (2013). STAR: Ultrafast universal RNA-seq aligner. Bioinformatics *29*,
910 15–21.

911 91. Love, M.I., Huber, W., and Anders, S. (2014). Moderated estimation of fold change and
912 dispersion for RNA-seq data with DESeq2. Genome Biology *15*, 1–21.

913 92. Mi, H., Ebert, D., Muruganujan, A., Mills, C., Albou, L.-P.P., Mushayamaha, T., and Thomas,
914 P.D. (2021). PANTHER version 16: A revised family classification, tree-based classification
915 tool, enhancer regions and extensive API. Nucleic Acids Research *49*, D394–D403.

916 93. Ishizaki, K., Chiyoda, S., Yamato, K.T., and Kohchi, T. (2008). Agrobacterium-mediated
917 transformation of the haploid liverwort *Marchantia polymorpha* L., an emerging model for
918 plant biology. Plant and Cell Physiology *49*, 1084–1091.

919 94. Kubota, A., Ishizaki, K., Hosaka, M., and Kohchi, T. (2013). Efficient Agrobacterium-
920 mediated transformation of the liverwort *Marchantia polymorpha* using regenerating thalli.
921 Bioscience, Biotechnology and Biochemistry *77*, 167–172.

922 95. Herrfurth, C., and Feussner, I. (2020). Quantitative Jasmonate Profiling Using a High-
923 Throughput UPLC-NanoESI-MS/MS Method. In Jasmonate in Plant Biology, Methods in
924 Molecular Biololgy, A. Champion and L. Laplaze, eds. (Humana, New York, NY), pp. 169–
925 187.

926 96. Ono, K., Ohyama, K., and Gamborg, O.L. (1979). Regeneration of the liverwort *Marchantia*
927 *polymorpha* L. From protoplasts isolated from cell suspension culture. Plant Science Letters
928 *14*, 225–229.

929 97. Takenaka, M., Yamaoka, S., Hanajiri, T., Shimizu-Ueda, Y., Yamato, K.T., Fukuzawa, H., and
930 Ohyama, K. (2000). Direct transformation and plant regeneration of the haploid liverwort
931 Marchantia polymorpha L. Transgenic Research *9*, 179–185.

932 98. Montgomery, S.A., Tanizawa, Y., Galik, B., Wang, N., Ito, T., Mochizuki, T., Akimcheva, S.,
933 Bowman, J.L., Cognat, V., Maréchal-Drouard, L., et al. (2020). Chromatin Organization in
934 Early Land Plants Reveals an Ancestral Association between H3K27me3, Transposons, and
935 Constitutive Heterochromatin. Current Biology *30*, 573-588.e7.

936

Figure 1

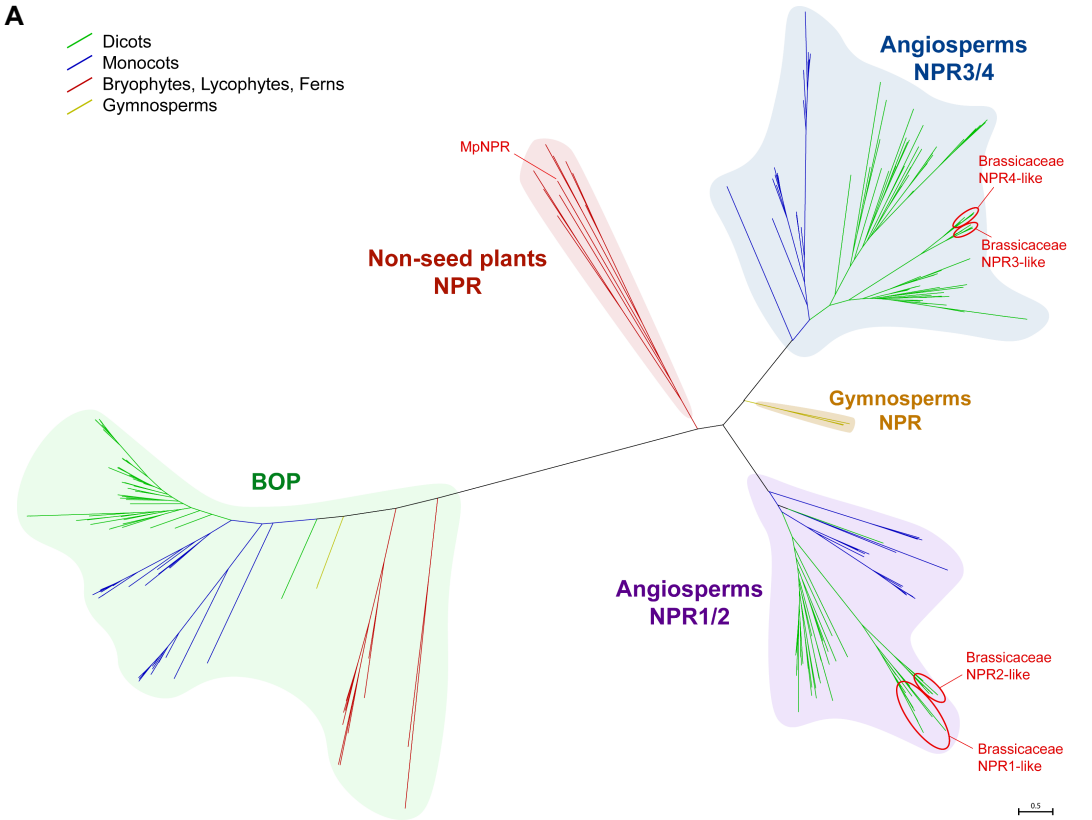
A
Dicots
Monocots
Bryophytes, Lycophytes, Ferns
Gymnosperms
Angiosperms NPR3/4
MpNPR
Brassicaceae NPR4-like
Brassicaceae NPR3-like
Non-seed plants NPR
Gymnosperms NPR
BOP
Angiosperms NPR1/2
Brassicaceae NPR2-like
Brassicaceae NPR1-like
0.5

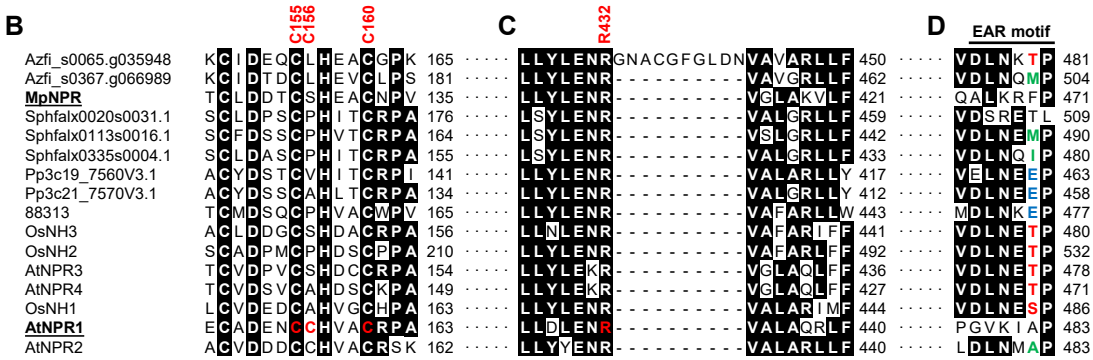
B
C155
C156
C160
C
R432
D
EAR motif
Azfi_s0065.g035948 KCIDEQCLHEACGPK 165 LLYLENRGNACGFGLDNVAVARLLF 450 VDLNKTP 481
Azfi_s0367.g066989 KCIDTDCLHEVCLPS 181 LLYLENR----------VAVGRLLF 462 VDLNQMP 504
MpNPR TCLDDTCSHEACNPV 135 LLYLENR----------VGLAKVLF 421 QALKRFP 471
Sphfalx0020s0031.1 SCLDPSCPHITCRPA 176 LSYLENR----------VALGRLLF 459 VDSRETL 509
Sphfalx0113s0016.1 SCFDSSCPHVTCRPA 164 LSYLENR----------VSLGRLLF 442 VDLNEMP 490
Sphfalx0335s0004.1 SCLDASCPHITCRPA 155 LSYLENR----------VALGRLLF 433 VDLNQIP 480
Pp3c19_7560V3.1 ACYDSTCVHITCRPI 141 LLYLENR----------VALARLLY 417 VELNEEP 463
Pp3c21_7570V3.1 ACYDSSCAHLTCRPA 134 LLYLENR----------VALGRLLY 412 VDLNEEP 458
88313 TCMDSQCPHVACWPV 165 LLYLENR----------VAFARLLW 443 MDLNKEP 477
OsNH3 ACLDDGCSHDACRPA 156 LLNLENR----------VAFARIFF 441 VDLNETP 480
OsNH2 SCADPMCPHDSCPPA 210 LLYLENR----------VAFARLFF 492 VDLNETP 532
AtNPR3 TCVDPVCSHDCCRPA 154 LLYLEKR----------VGLAQLFF 436 VDLNETP 478
AtNPR4 TCVDSVCAHDSCKPA 149 LLYLEKR----------VGLAQLFF 427 VDLNETP 471
OsNH1 LCVDEDCAHVGCHPA 163 LLYLENR----------VALARIMF 444 VDLNESP 486
AtNPR1 ECADENCCHVACRPA 163 LLDLENR----------VALAQRLF 440 PGVKIAP 483
AtNPR2 ACVDDDCCHVACRSK 162 LLYYENR----------VALARLLF 440 LDLNMAP 483

Figure 2

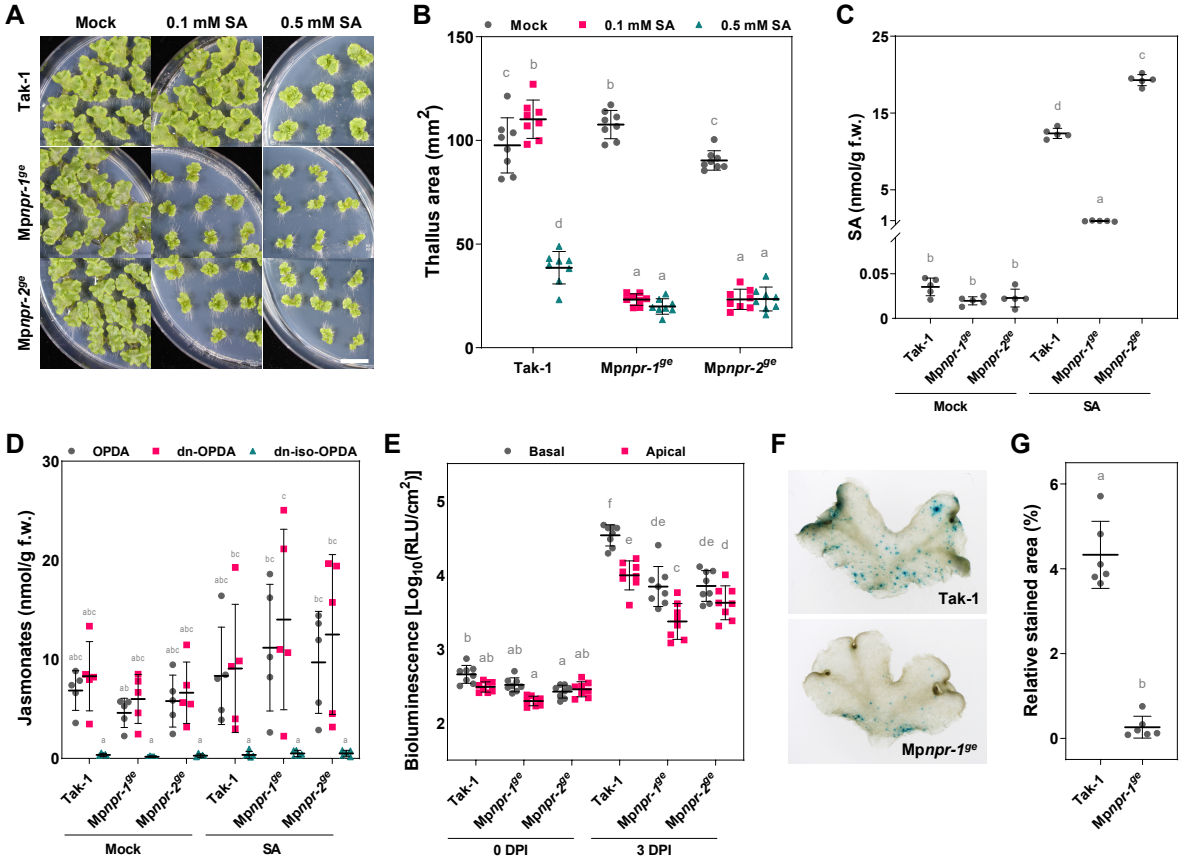
A
Mock
0.1 mM SA
0.5 mM SA
Tak-1
Mpnpr-1ge
Mpnpr-2ge
B
Mock
0.1 mM SA
0.5 mM SA
Thallus area (mm2)
150
100
50
0
Tak-1
Mpnpr-1ge
Mpnpr-2ge
C
SA (nmol/g f.w.)
25
15
5
1
0.05
0
Tak-1
Mpnpr-1ge
Mpnpr-2ge
Mock
SA
D
OPDA
dn-OPDA
dn-iso-OPDA
Jasmonates (nmol/g f.w.)
30
20
10
0
Tak-1
Mpnpr-1ge
Mpnpr-2ge
Mock
SA
E
Basal
Apical
Bioluminescence [Log10(RLU/cm2)]
5
4
3
2
Tak-1
Mpnpr-1ge
Mpnpr-2ge
0 DPI
3 DPI
F
Tak-1
Mpnpr-1ge
G
Relative stained area (%)
6
4
2
0
Tak-1
Mpnpr-1ge

Figure 3

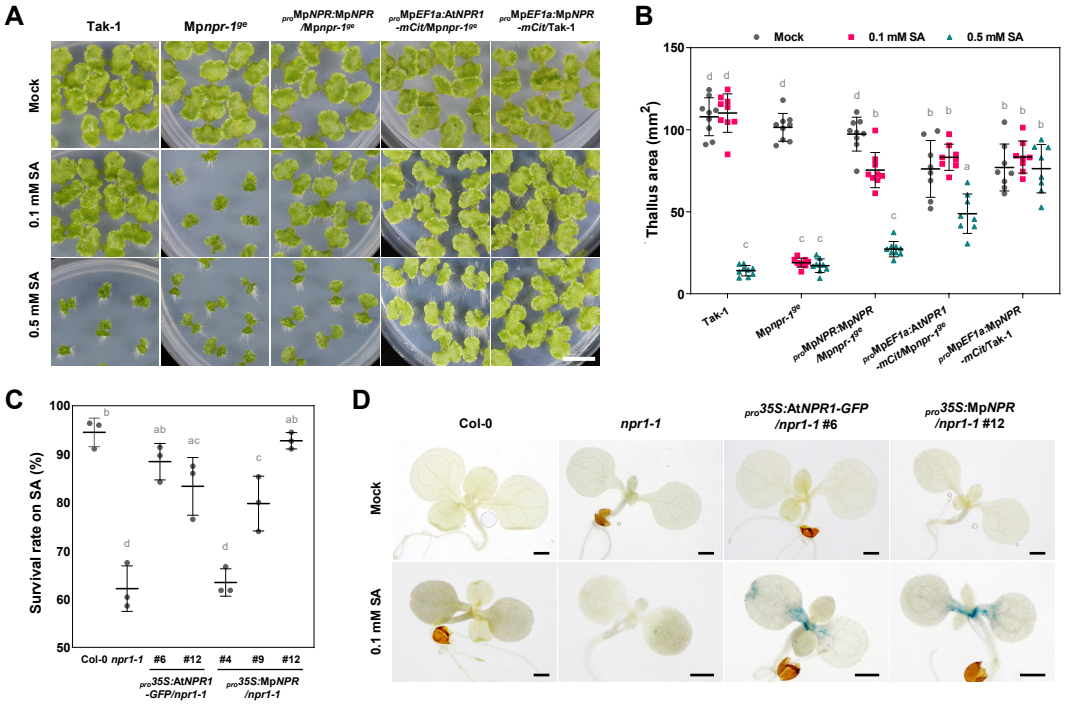
A
Tak-1
Mpnpr-1ge
proMpNPR:MpNPR /Mpnpr-1ge
proMpEF1a:AtNPR1 -mCit/Mpnpr-1ge
proMpEF1a:MpNPR -mCit/Tak-1
Mock
0.1 mM SA
0.5 mM SA
B
Mock
0.1 mM SA
0.5 mM SA
Thallus area (mm2)
150
100
50
0
Tak-1
Mpnpr-1ge
proMpNPR:MpNPR /Mpnpr-1ge
proMpEF1a:AtNPR1 -mCit/Mpnpr-1ge
proMpEF1a:MpNPR -mCit/Tak-1
C
Survival rate on SA (%)
100
90
80
70
60
50
Col-0
npr1-1
#6
#12
#4
#9
#12
pro35S:AtNPR1 -GFP/npr1-1
pro35S:MpNPR /npr1-1
D
Col-0
npr1-1
pro35S:AtNPR1-GFP /npr1-1 #6
pro35S:MpNPR /npr1-1 #12
Mock
0.1 mM SA

Figure 4

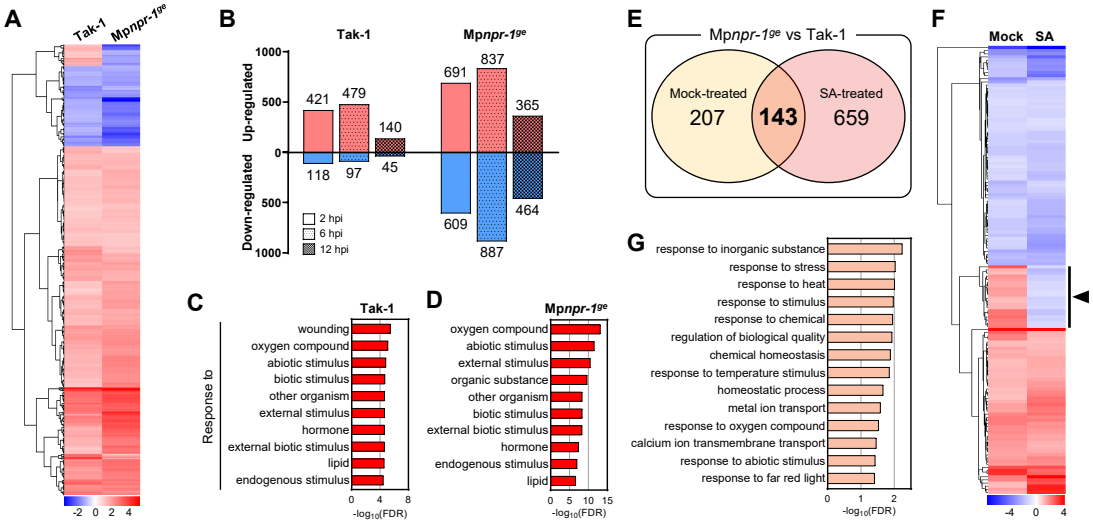
A
Tak-1
Mpnpr-1ge
-2 0 2 4
B
Tak-1
Mpnpr-1ge
Up-regulated
Down-regulated
1000
500
0
500
1000
421
479
140
118
97
45
691
837
365
609
887
464
2 hpi
6 hpi
12 hpi
C
Tak-1
Response to
wounding
oxygen compound
abiotic stimulus
biotic stimulus
other organism
external stimulus
hormone
external biotic stimulus
lipid
endogenous stimulus
0 4 8
-log10(FDR)
D
Mpnpr-1ge
oxygen compound
abiotic stimulus
external stimulus
organic substance
other organism
biotic stimulus
external biotic stimulus
hormone
endogenous stimulus
lipid
0 5 10 15
-log10(FDR)
E
Mpnpr-1ge vs Tak-1
Mock-treated
207
143
SA-treated
659
G
response to inorganic substance
response to stress
response to heat
response to stimulus
response to chemical
regulation of biological quality
chemical homeostasis
response to temperature stimulus
homeostatic process
metal ion transport
response to oxygen compound
calcium ion transmembrane transport
response to abiotic stimulus
response to far red light
0 1 2
-log10(FDR)
F
Mock
SA
-4 0 4

Figure 5

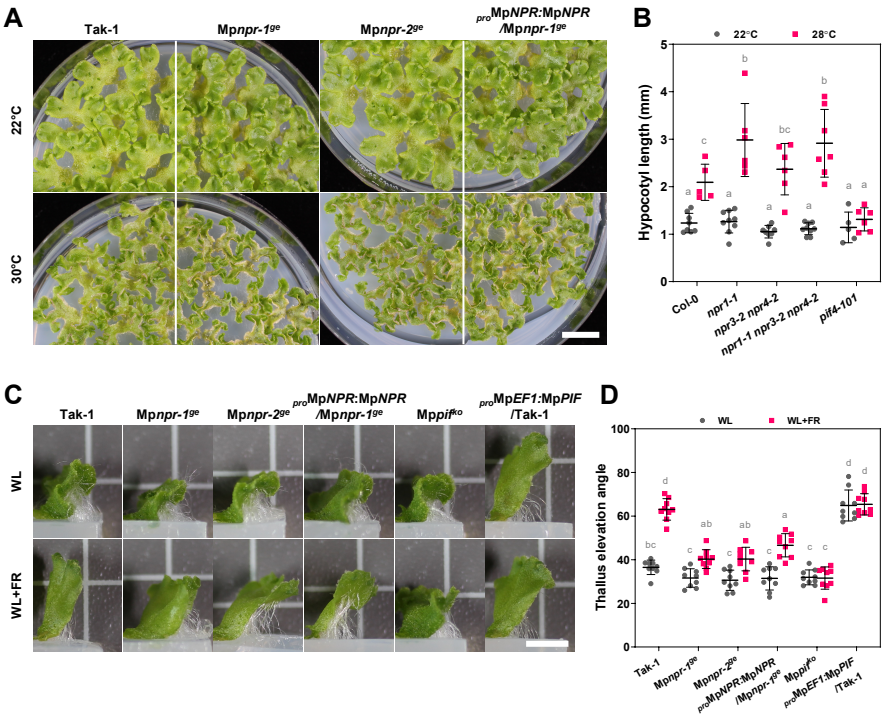
A
Tak-1
Mpnpr-1ge
Mpnpr-2ge
proMpNPR:MpNPR /Mpnpr-1ge
22°C
30°C
B
22°C
28°C
Hypocotyl length (mm)
Col-0
npr1-1
npr3-2 npr4-2
npr1-1 npr3-2 npr4-2
pif4-101
C
Tak-1
Mpnpr-1ge
Mpnpr-2ge
proMpNPR:MpNPR /Mpnpr-1ge
Mppifko
proMpEF1:MpPIF /Tak-1
WL
WL+FR
D
WL
WL+FR
Thallus elevation angle
Tak-1
Mpnpr-1ge
Mpnpr-2ge
proMpNPR:MpNPR /Mpnpr-1ge
Mppifko
proMpEF1:MpPIF /Tak-1

Supplementary Figure S1

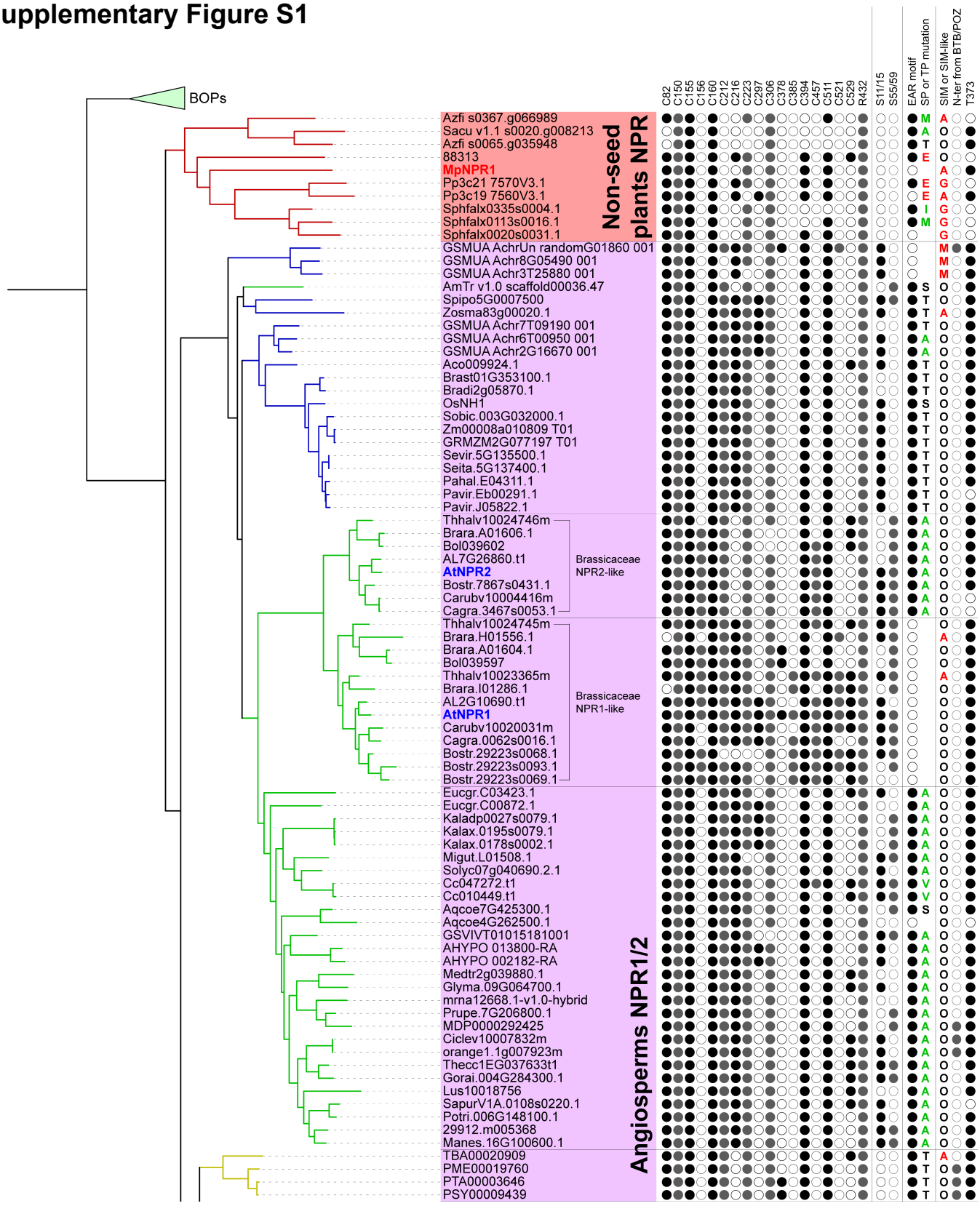

Supplementary Figure S1. Phylogenetic tree showing the conservations of functional residues and motifs of 194 NPR proteins, related to Figure 1.

Presence and absence of functional residues and motifs are shown by closed and open circle, respectively. In SP/TP mutations, substitutions with non-phosphorylatable hydrophobic residues (A/V/L/I/M) are colored in green.

Supplementary Figure S1 (Continued)

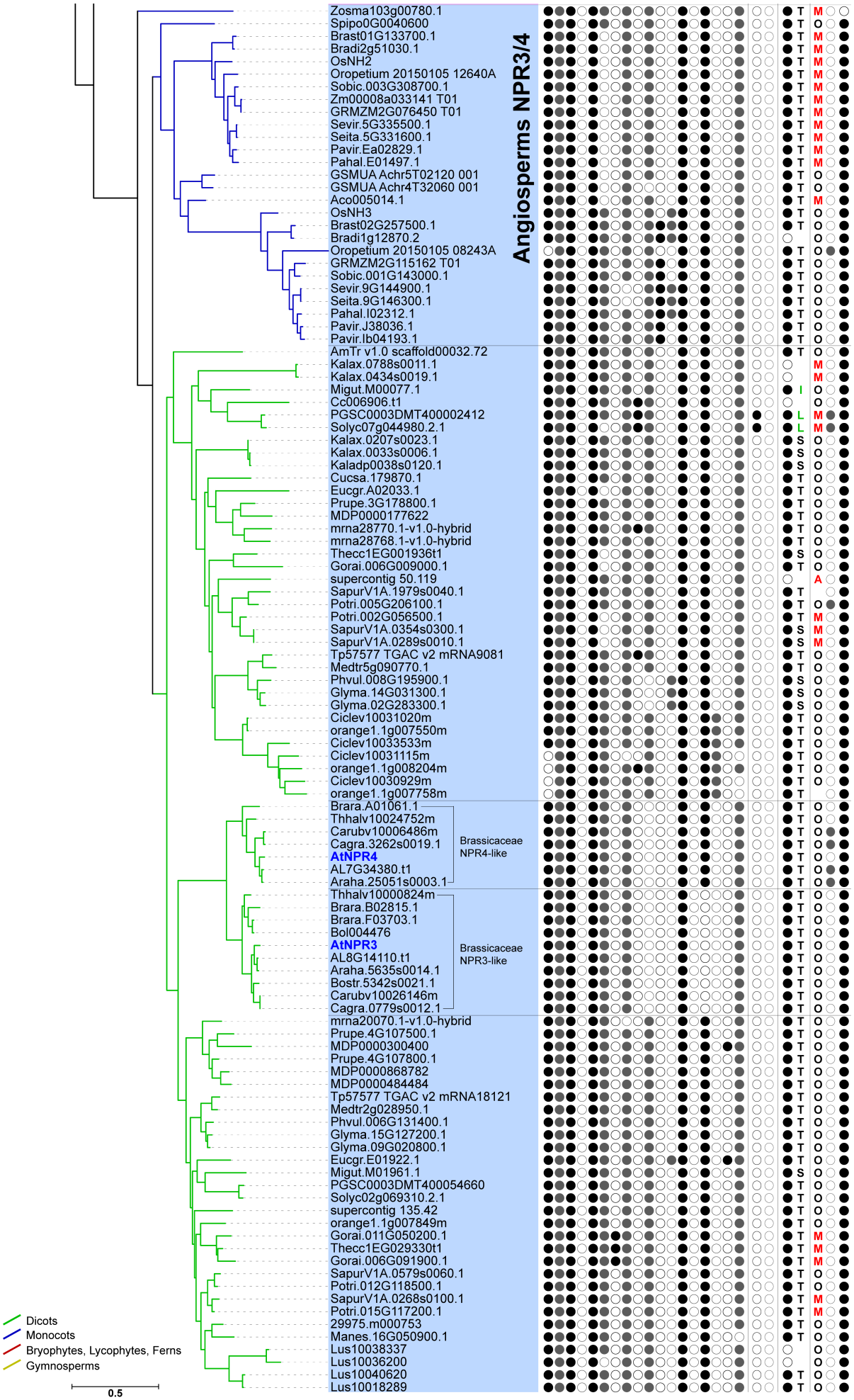

Supplementary Figure S2

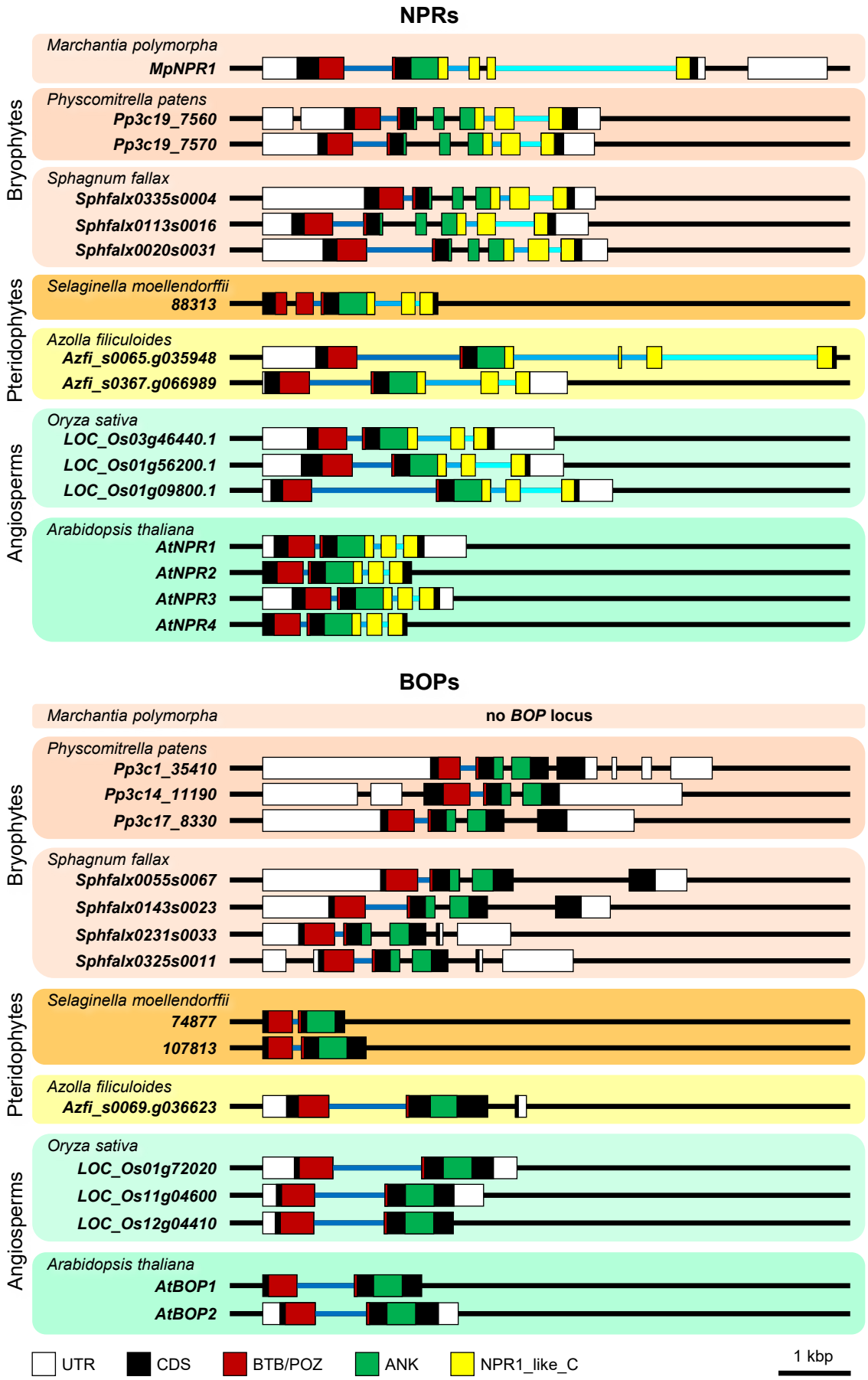

Supplementary Figure S2. The exon-intron organization in the BTB/POZ-encoding regions are highly conserved between NPR and BOP families

Supplementary Figure S3

A

	NPR1	NPR2	NPR3	NPR4
Arabidopsis halleri	1	1	1	1
Arabidopsis lyrata	1	1	1	1
Arabidopsis thaliana	1	1	1	1
Boechera stricta	4	1	1	1
Brassica oleracea capitata	1	1	1	0
Brassica rapa FPsc	3	1	2	1
Capsella grandiflora	1	1	1	1
Capsella rubella	1	1	1	1
Eutrema salsugineum	2	1	1	1

B

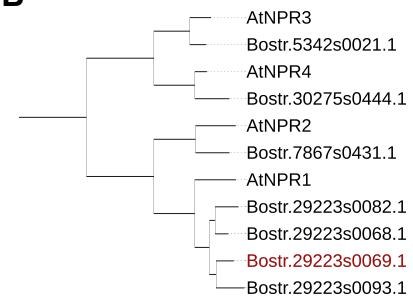

C

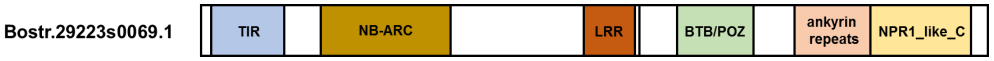

Supplementary Figure S3. Gene duplications in Brassicaceae-specific NPR subclades and integration of *Boechera stricta* NPR1 homolog into TIR-NLR protein, related to Figure 1A.

(A) Number of NPRs in Brassicaceae species suggesting the selective pressures or expansions of Brassicaceae NPR-like genes. (B) Phylogenetic analysis of *Boechera stricta* NPR homologs. (C) Schematic of domains showing that Bostr.29223s0069.1 is integrated into the C-terminus of TIR-NLR proteins in *Boechera stricta*.

Supplementary Figure S4

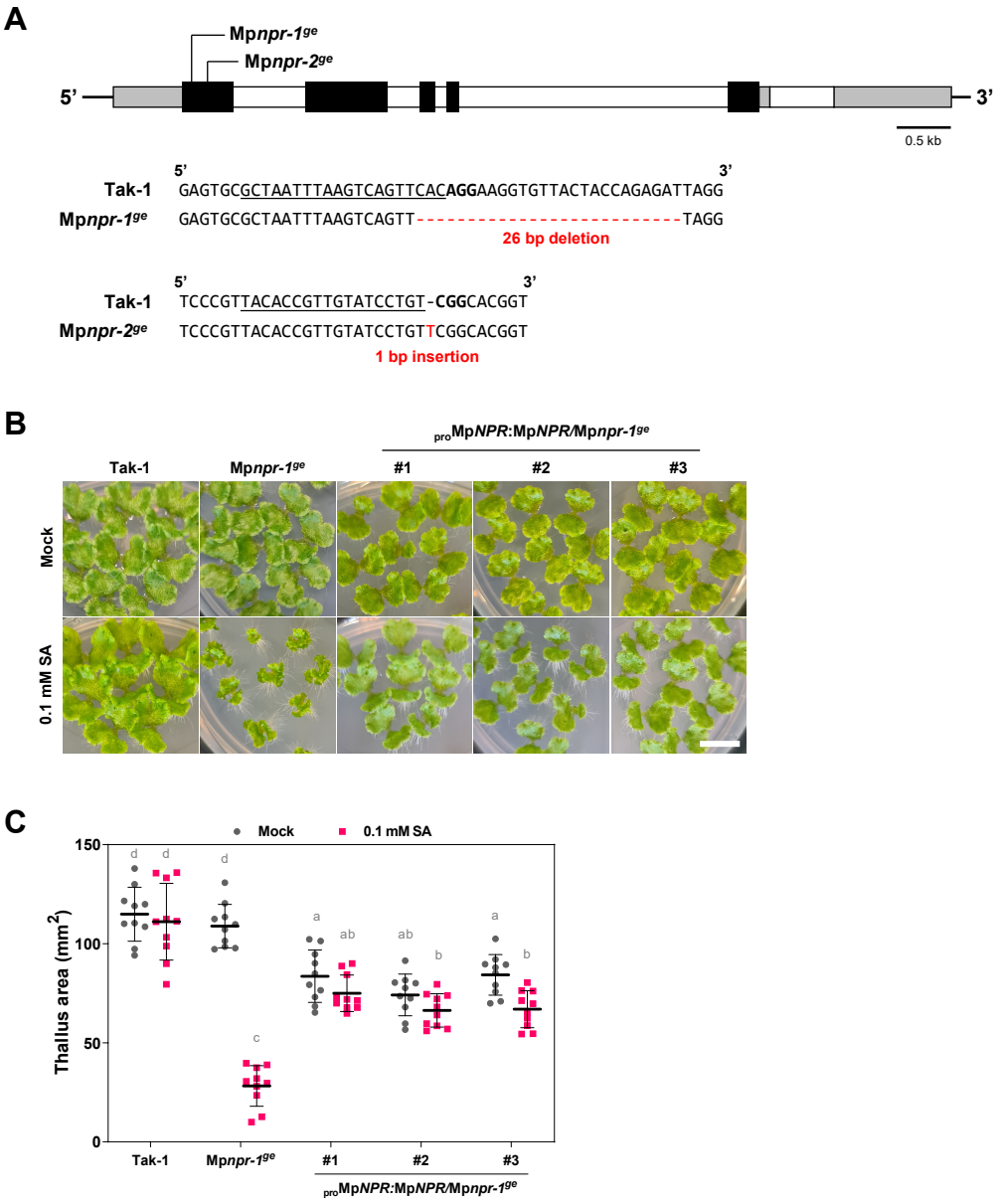

Supplementary Figure S4. Generation of Mp*npr* mutants using CRISPR/Cas9 system and complementation of the SA-hypersensitivity phenotype in the mutants.

(A) Schematic of sgRNA target sites in the first exon of Mp*NPR*. Black, white and gray boxes indicate exons, introns, and UTRs, respectively. Mp*npr-1*^{ge} and Mp*npr-2*^{ge} resulted in 26 bp deletion and 1 bp insertion, respectively. (B) Complementation of SA-hypersensitivity in individual transgenic lines expressing $_{pro}$Mp*NPR*:Mp*NPR*. Two-week-old *M. polymorpha* grown on mock and 0.1 mM SA conditions are shown. Scale bar, 1 cm. (C) Quantification of thallus projected area shown in B. Different letters represent statistical significances (Tukey's test; $p < 0.01$). Error bars indicate SD (n = 10).

Supplementary Figure S5

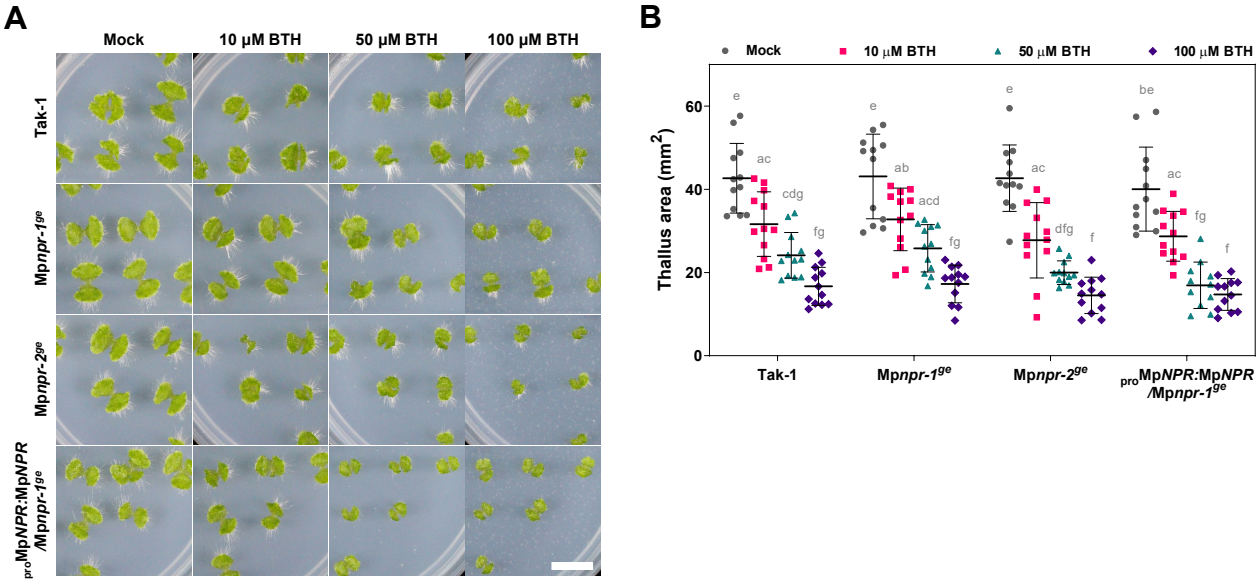

Supplementary Figure S5. BTH sensitivity was unchanged in Mp*npr* mutants compared to Tak-1.

(A) Ten-day-old *M. polymorpha* grown BTH conditions showing that BTH sensitivity was unchanged in Mp*npr* mutants compared to Tak-1. Scale bar, 1 cm. (B) Quantification of thallus projected area shown in A. Different letters represent statistical significances (Tukey's test; $p < 0.01$). Error bars indicate SD (n = 12).

Supplementary Figure S6

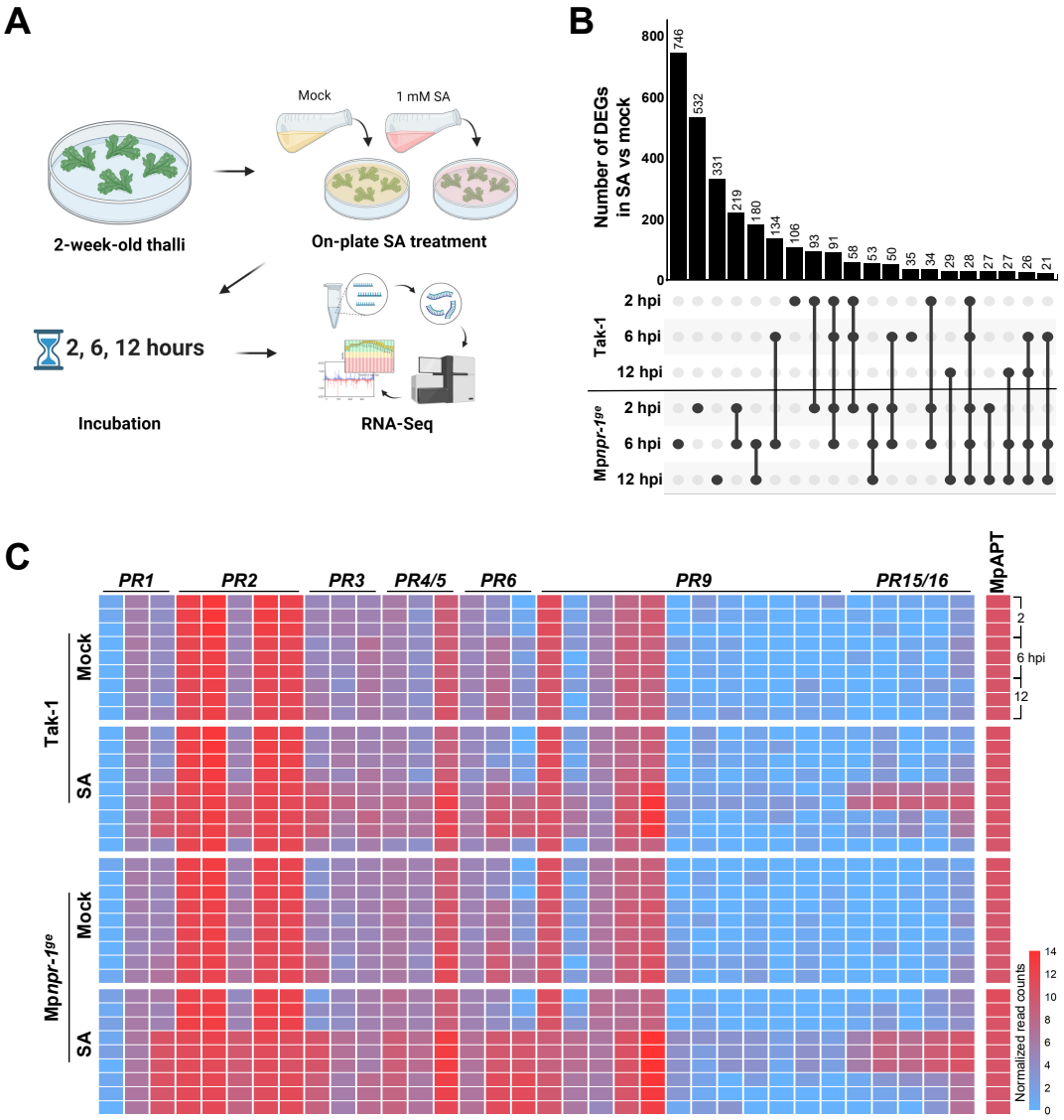

Supplementary Figure S6. RNA-Seq analysis comparing Tak-1 and Mp*npr-1*^{ge} thalli in Mock and SA conditions.
(A) Schematic of thalli preparation for RNA-Seq analysis. (B) UpSet plot showing the number of unique and conserved DEGs (Mock vs SA, |Log2FC| ≥ 1, adjusted $p < 0.05$) in each dataset. Linked dots indicate that datasets share the DEGs. Comparisons showing more than 20 DEGs are shown. (C) Heatmap of selected Mp*PR* gene expressions in individual samples.

Supplementary Figure S7

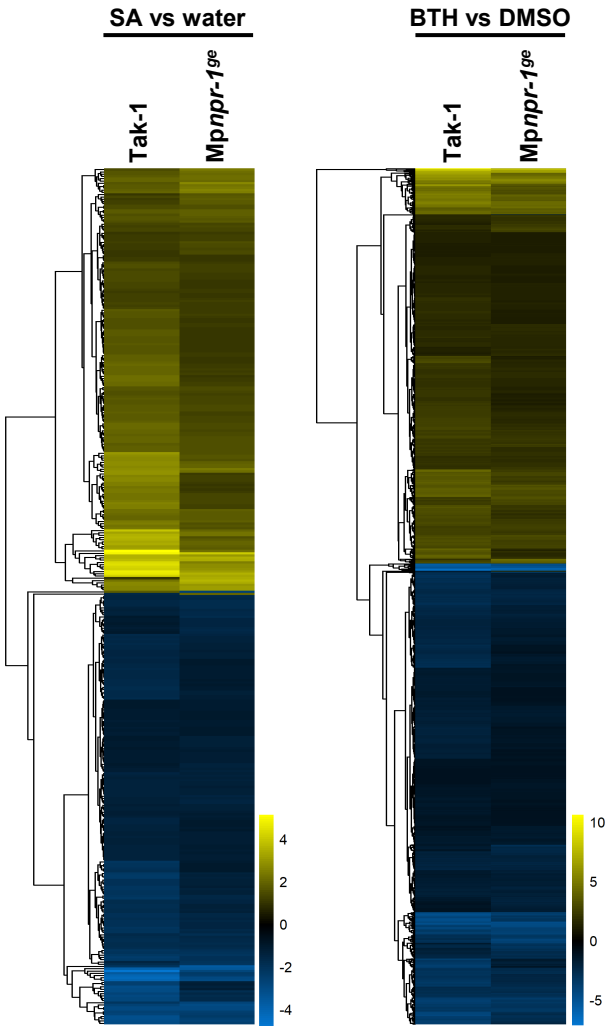

Supplementary Figure S7. RNA-Seq analysis comparing Tak-1 and Mp*npr-1*^{ge} gemmae in Mock, SA, and BTH conditions.

Heatmap of DEGs (|log2FC| ≥ 1, adjusted p < 0.05) in Tak-1 and Mp*npr-1*^{ge} gemmae upon SA (left) and BTH (right) treatments compared to each mock conditions.